C.P. No. 571

C.P. No. 571

MINISTRY OF AVIATION

AERONAUTICAL RESEARCH COUNCIL

CURRENT PAPERS

Low-Speed Wind Tunnel Tests on the Effects of Taper on Low Aspect-Ratio Wings at Zero Incidence

by

D. H. Peckham, B.Sc., A.F.R.Ae.S.

LONDON: HER MAJESTY'S STATIONERY OFFICE

1961

SIX SHILLINGS NET

U.D.C. No. 533.693.3 : 533.69.031 : 533.69.048.2

C.P. No.571

August, 1960.

LOW-SPEED WIND TUNNEL TESTS ON THE EFFECTS OF TAPER ON LOW ASPECT-RATIO WINGS AT ZERO INCIDENCE

by

D. H. Peckham, B.Sc., A.F.R.Ae.S.

SUMMARY

A family of low aspect ratio wings of RAE 101 section, and one of biconvex section, have been tested in the 13 ft x 9 ft low-speed wind tunnel at RAE Bedford.

Results of pressure measurements at zero incidence are analysed to determine the separate effects of low aspect-ratio, thickness taper, planform taper and sweep on the chordwise velocity distributions.

Previously issued as R.A.E. Tech. Note No. Aero.2710 - A.R.C. 22,506.

LIST OF CONTENTS

LIST OF TABLES

LIST OF ILLUSTRATIONS

LIST OF ILLUSTRATIONS (CONTD)

1 INTRODUCTION

With the modern trend towards wings of low aspect ratio, the effects of "planform taper" and "thickness taper" have become more marked, the two types of taper being defined in the following way:-

Planform taper The decrease of wing chord across the span, (without implying a corresponding variation of wing thickness).

Thickness taper The decrease of wing maximum thickness across the span; (not the spanwise variation of thickness/chord ratio).

At zero incidence, thickness taper usually results in a decrease in the velocities over the inboard parts of the wing, relative to a wing of the same planform and centre-section thickness/chord ratio; while planform taper causes an increase in the velocities over the outboard parts, relative to an untapered wing of the same mean sweep. To take the fullest advantage of these effects, it is important that the separate contributions of planform taper and thickness taper to the velocities on a wing are accurately known for various angles of sweep. Since thickness taper allows a high wing-root thickness without causing high velocities at the root, it might be profitably employed for the following reasons:-

(a) To concentrate the enclosed volume of the wing near the wing-root,

(b) To give a better junction shape with a fuselage

and (c) To allow a high spar depth at the wing-root.

Furthermore it has been shown in Ref. 1 that certain sharp-edged slender wings with a high rate of thickness taper at the root, have geometric characteristics which could simplify the design and construction of both full-size aircraft and wind-tunnel models. These wings are also of special interest aerodynamically, in that the calculation of the velocity distributions on their surfaces is straightforward.

In a theoretical study, Newby[2] has considered a number of wings of simple planform shape with biconvex sections, and obtained quantitative results for the separate effects of planform taper, thickness taper and sweep on their velocity distributions at zero incidence. These results were then related to the standard chordwise distributions for the infinite sheared wing, and the centre section of the infinite swept wing, by velocity increments depending on planform taper, thickness taper and sweep. It was then assumed that the same increments could be retained for wings of any chordwise profile where the two standard distributions were known. However, these results for wings of biconvex section could not be applied with certainty to wings with round-nosed aerofoil sections, since very little experimental evidence was available in a form suitable for analysis.

For this reason a family of wings of various tapers has been tested to determine how far the results obtained by Newby can be used quantitatively for wings of symmetrical round-nosed section (in this case RAE 101). A single model of biconvex parabolic-arc section was also included in the tests to enable a direct comparison to be made with theory. Although only zero incidence velocity distributions were required for comparison with theory, a small incidence range was covered to obtain local section characteristics, and overall force and moment measurements*. Some results

* Tabulated lists of pressure coefficients and integrated sectional force coefficients at incidences other than zero are not included in this Note.

of tests on slender wings with sharp edges, reported in Ref. 5, are also included to provide information on wings of lower aspect ratio than the family of round-nosed wings tested. Theoretical work by Neumark and Collingbourne[3], and Weber[4], has been compared with the experimental results in cases where applicable.

2 DESCRIPTION OF MODELS AND TESTS

The family of wings tested consisted of eight models of RAE 101 section, with 30 in. root chord and 42 in. span, the thickness/chord ratio at the centre line being 12% in all cases. Four wings were of constant chord, and four of planform taper ratio zero, giving aspect ratios of 1.4 and 2.8 respectively. Details of the models are shown in Figs. 1 and 2. As the wings all had the same span/root chord ratio and root section, their geometry is defined by:-

(a) Planform taper ratio (1 or 0) equal to tip chord/root chord

(b) Tip thickness/chord ratio $\mu\left(\frac{t_o}{c_o}\right)$, μ being either 1 or 0. ($\mu = 1$ means zero thickness taper on the wings of constant chord, and linear thickness taper on the wings of zero planform taper ratio. Similarly $\mu = 0$ means either linear thickness taper or parabolic thickness taper.)

(c) Sweep of 30% chord line, ϕ_k; this is effectively the sweep of the maximum thickness line (which is actually at 31% chord).

From this family of eight wings the following separate effects of planform taper, thickness taper and sweep on the velocities on the wings at zero incidence have been found:-

(a) Wings 1 and 2. The effect of thickness taper on constant chord wings of zero sweep.

(b) Wings 3 and 4. The effect of thickness taper on constant chord wings of 45° sweep.

(c) Wings 1 and 3, 2 and 4. The effect of sweep on constant chord wings of the same thickness taper.

(d) Wings 5, 6 and 8. Effect of sweep on wings of zero planform taper ratio, and linear thickness taper.

(e) Wings 6 and 7. Effect of thickness taper on 45° swept wings of zero planform taper ratio.

(f) Wings 2 and 5. Effect of planform taper ratio on unswept wings of linear thickness taper.

(g) Wings 4 and 6. Effect of planform taper ratio on 45° sweep wings of linear thickness taper.

The wing with parabolic-arc sections was included to obtain a direct comparison with theory, and was similar to wing 5, except that the unswept maximum thickness line was at 50% chord. Results of pressure measurements at zero incidence on two delta wings of aspect ratio 1, with parabolic-arc sections, are also included. Details of these three models are shown in Fig. 3.

All measurements were made at a tunnel speed of 200 ft/sec, which gave a Reynolds number of 3.14×10^6 (based on root chord) for wings 1-8 and wing A.

3 SUPERVELOCITY DISTRIBUTIONS AT ZERO INCIDENCE, WINGS 1-8

3.1 General

The results of pressure measurements at zero incidence (Table 1) are plotted as supervelocities, which are directly proportional to the thickness/chord ratio t_o/c_o, (at least up to moderate thickness/chord and nose-radius/chord ratios). The supervelocity, v_x, is related to the pressure coefficient by:-

$$\frac{v_x}{V_o} = \sqrt{1 - C_p} - 1$$

where V_o is the free stream velocity.

In Ref. 2, the supervelocities are plotted in the form:-

$$\frac{\pi}{4 V_o (t_o/c_o)} \cdot \frac{v_x}{V_o}$$

the significance of this expression being that it is equal to unity at the maximum-thickness position on a two-dimensional wing of biconvex parabolic-arc section at zero incidence.

The velocity increments due to the effects of taper derived in Ref. 2, are based on calculations made for wings of biconvex parabolic-arc section, where the maximum thickness position is at 50% chord. It was estimated (by combining suitable parabolic-arcs) that the effect of moving the maximum thickness position forward from 50% to 33⅓% chord would be to increase the supervelocity there by about 30% on rectangular wings (Fig. 6(a), Ref. 2), and about 15% on wings tapered in plan (Fig. 23(a), Ref. 2). Another theoretical estimate of the effect of maximum thickness position has been made for rectangular wings by Weber[4], which gives a supervelocity at the maximum thickness position on a wing of RAE 101 section (t_{max} at 31% chord) about 15% above that of a comparable wing of biconvex parabolic-arc section. The latter figure was confirmed by the results obtained from wing 1, and in Fig. 4 it can be seen that excellent agreement with theory is obtained. Clearly, it is not accurate enough simply to approximate a round-nosed aerofoil section by combining two parabolic-arcs to give the same maximum thickness position, as was attempted in Ref. 2. Hence, where the results of the present series of tests on wings of RAE 101 section are compared with the theoretical estimates of Ref. 2, the experimental results have been reduced by the factor $F = v_x(k)$ biconvex$/v_x(k)$ RAE 101 = 1/1.15. The values of the supervelocity are therefore plotted as:-

$$F \cdot \frac{\pi}{4 V_o (t_o/c_o)} \cdot \frac{v_x}{V_o}$$

it is, of course, possible for results for wings of any section to be compared with the theoretical values in Ref. 2, provided that the ratio F is known.

3.2 Effect of finite span

The effects of finite span on unswept and swept wings of constant chord, and constant thickness/chord ratio, are illustrated in Figs. 5 and 6 respectively. The results are in good agreement with the estimates made by Newby (Fig. 7), and confirm that at low aspect ratios and angles of sweep, finite span causes an appreciable reduction in the supervelocity at the centre section, but that the effect diminishes with increase of sweep becoming almost negligible when a sweep of 45° is reached.

3.3 Effects of thickness taper

Plotted in Figs. 8 and 9 are the chordwise supervelocity distributions at various spanwise positions on two rectangular wings of different thickness tapers; one a wing of constant spanwise thickness distribution, the other tapered linearly in thickness over its whole span. For each wing a unique curve of $v_x(x)/v_x(k)$ is obtained, where $v_x(k)$ is the supervelocity at the maximum thickness position. For the wing of constant thickness, this curve is similar in shape to the chordwise distribution for the two-dimensional wing, but on the other the effect of the thickness taper alters the shape of the distribution from that of the two-dimensional case. Thus the chordwise supervelocity distributions on the wing of RAE 101 section tapered in thickness cannot be accurately obtained by scaling the distribution for the two-dimensional wing by an appropriate factor, τ, as suggested in Ref. 2 for wings with biconvex profiles.

Also plotted in Figs. 8 and 9 are the theoretical centre-line supervelocity distributions of Weber[4]. Excellent agreement is obtained between theory and the experimental results for the wing of constant thickness/chord ratio, but for wing 2, theory slightly underestimates the reduction in supervelocity due to the thickness taper; however, the shape of the theoretical distribution is correct.

The effect of thickness taper in reducing the supervelocity at the maximum thickness line of a rectangular wing, relative to that on the two-dimensional wing of the same local thickness/chord ratio, is illustrated in Fig. 10(a). Part of this reduction is solely the effect of reduced thickness/chord ratio, but Fig. 10(b) shows the reduction on the basis of the local thickness/chord ratio. It can be seen that the maximum effect of the thickness taper is at the centre-section of the wing, the reduction of supervelocity decreasing almost linearly, becoming zero and changing sign at about $\eta = 0.8$.

From the above it is apparent that a close estimate of the chordwise supervelocity distribution at any spanwise position on a rectangular wing tapered in thickness, can be obtained by using the theory of Weber[4] to obtain the distribution at the wing centre-line, and reducing this by the appropriate amount (given by the theory of Ref. 2) to obtain the distribution at other spanwise positions.

Supervelocity distributions on a constant chord, constant thickness/chord ratio, wing of 45° sweep are shown in Fig. 11. Here again, the experimental distribution at the wing centre-line agrees well with the theory of Ref. 4. Results for a similar wing, but tapered linearly in thickness, are given in Fig. 12. These swept wings are of the same aspect ratio as the rectangular wings (1 and 2), but it is found that the reduction in supervelocity at the maximum thickness line, due to the effects of the thickness taper, is less than on the corresponding unswept wings (Fig. 13). This decrease in the effect of thickness taper with increase of sweep was predicted by the theory of Ref. 2; the experimental values of this reduction

at the maximum thickness position on the wing centre-lines are compared with the theoretical values in Figs. 13 and 14.

The effect of different rates of thickness taper on wings also tapered in planform is illustrated by comparing results for wings 6 and 7, which are deltas of aspect ratio 2.8, the former tapering linearly in thickness from the root, while the latter decreases parabolically in thickness from the root. Results for these wings are plotted in Figs. 16 and 17, and analysis shows the two main effects of thickness taper found previously with the constant-chord wings. (Fig. 18). Firstly, the higher rate of thickness taper causes a reduction in supervelocity at the wing centre section with only a slight effect on the shape of the chordwise distribution, the $\frac{v_x(x)}{v_x(k)}$ curves for each wing being very similar (Fig. 18(a)). Secondly a comparison of the supervelocity distributions at the maximum thickness lines of the wings, on the basis of local thickness/chord ratio, reveals that the effect of the higher rate of thickness taper is only apparent near the centre of the wing (out to $\eta = 0.3$); the same effect was found with the constant-chord wings of 45° sweep, which was also the sweep of the maximum thickness line of these delta wings.

3.4 Effects of planform taper

Plotted in Fig. 15 are the chordwise supervelocity distributions on wing 5, which is tapered linearly both in plan and thickness, and is unswept at the maximum thickness line. Over the region covered by the pressure-plotting tests ($0 < \eta < 0.3$), the shape of the chordwise supervelocity distribution remains the same. Comparison with the results for wing 2, a rectangular wing but of the same thickness taper, reveals that planform taper has the following effects:-

(i) At the centre section of the wing, the peak value of the supervelocity is almost unchanged but the shape of the chordwise distribution is altered, the supervelocities on the wings tapered in planform becoming progressively less towards the leading and trailing edges than those on the rectangular wing of the same thickness distribution. These effects were predicted in the theory of Ref. 2, though at very low aspect ratios it was expected that planform taper would increase the supervelocity at the centre-section maximum thickness position by a small amount. The results in fact show this, but a firm conclusion cannot be drawn because the difference is of the same order as the possible experimental error.

(ii) At the spanwise maximum thickness line the supervelocities become greater towards the wing tip, while on the rectangular wing tapered in thickness the supervelocities steadily decrease towards the tip.

Similarly, the effects of planform taper on wings of 45° sweep at the maximum thickness line is shown by a comparison of the results for wings 4 and 6, which are plotted in Figs. 12 and 16. Here too, the effects noticed with the unswept wings are found, though the increase in supervelocity at the maximum thickness line due to planform taper is not as great as with the unswept wing.

3.5 Effects of sweep

The effect of sweep on wings tapered linearly both in plan and thickness is shown by comparing the results plotted in Figs. 19, 20 and 21, where the results are plotted for wings 5, 6 and 8 of 0°, 45° and 60° sweep at the maximum thickness line respectively. Increasing sweep is seen to have the effect of:-

(i) Reducing the peak supervelocity at the centre section, and altering the shape of the chordwise distribution so that the peak supervelocity occurs at a more rearward position.

(ii) Reducing the rate at which the supervelocities at the maximum thickness line increases with distance from the wing centre-line.

4 SUPERVELOCITY DISTRIBUTIONS AT ZERO INCIDENCE, WINGS A, B AND C

A single model of biconvex parabolic-arc section, wing A of Fig. 3, was included in the present series of tests in order to enable a direct comparison to be made with the theories of Newby[2], and Neumark and Collingbourne[3]. Results for two delta wings of aspect ratio 1, wings B and C of Fig. 3, are also included; tests on these are reported fully in Ref. 5. The pressure coefficients measured at zero incidence on wings A, B and C are given in Table 1.

Supervelocities at the maximum thickness line on wing A (at 50% chord) are compared with the theoretical prediction of Neumark and Collingbourne[3] in Fig. 22, (their value of the supervelocity at the maximum thickness position on the centre-section being in agreement with that given in Ref. 2). It is seen that the reduction of supervelocity at the centre-section, relative to the two-dimensional value, and the rate at which the supervelocities increase outboard of the centre-line, are greater than predicted by the theory of Ref. 3. Also plotted in Fig. 22 are the supervelocities on the corresponding wing (wing 5) of RAE 101 section, with an unswept maximum thickness line at 30% chord. Some chordwise supervelocity distributions on wing A are plotted in Fig. 23, and in Fig. 24 the theoretical and experimental reductions of supervelocity at the maximum thickness line of the wing are shown relative to the two-dimensional value for the local thickness/chord ratio.

The experimental supervelocity distributions on the centre-lines of wings B and C are compared with the theoretical estimates of Ref. 2 in Fig. 25. Here again, it is found that the experimental values are considerably less than those predicted by theory. Although the shape of the experimental distribution for wing B does not agree so well with the theoretical estimate as in the case of wing C, it should be noted that the theoretical distribution for wing B was determined from calculations for two wings whose mean thickness taper was approximately linear, and is therefore not such a reliable estimate. In addition, Ref. 2 assumes that the wing thickness is small compared with the span, which clearly does not hold here.

5 CONCLUSIONS

5.1 The present series of tests confirm the main qualitative effects of taper on wings of low aspect ratio at zero incidence which were predicted in Ref. 2.

5.2 Thickness taper has two main effects, which are:

(i) to reduce the velocities near the centre-section of the wing, the greatest reduction being at the centre-line.

(ii) to alter slightly the shape of the chordwise supervelocity distribution from that of the untapered wing.

The magnitude of these effects decreases with increase of sweep.

5.3 Planform taper has two main effects also, which are:-

(i) to increase the velocities outboard of the wing centre-section, there being a progressive increase towards the wing tip.

(ii) to alter the shape of the chordwise velocity distribution, although the magnitude of the maximum supervelocity at the centre-section is only slightly affected. It should be noted, though, that the theory of Ref. 2 predicts an increase of supervelocity at the centre-section for wings of aspect ratios lower than those of the wings in the present tests.

The magnitude of these effects decreases with increase of sweep.

5.4 The limited scope of the present tests did not enable the variation of the effects of taper with aspect ratio, and with spanwise extent of taper, to be investigated. However, the limited spot checks that could be made confirmed the theory of Ref. 2.

5.5 The assumption in Ref. 2 that - "for rectangular wings of symmetrical parabolic-arc aerofoil section, the supervelocity distributions are similar in shape to the corresponding two-dimensional distribution, but with the supervelocities at all points of the chord reduced in approximately the same ratio" - is not strictly justified for more conventional profiles in that thickness taper alters the shape of the chordwise distribution, as pointed out by Weber[4]. This raises a difficulty in presentation of results in that the reduction of supervelocity at the maximum thickness position is different from the reduction in peak supervelocity, the peak values on an untapered and a tapered wing not being at the same chordwise position. However, the estimates in Ref. 2 for the spanwise variation of supervelocity at the maximum thickness position on rectangular wings were confirmed by the present tests.

5.6 The theory of Ref. 4 gives close estimates of the centre-section distribution on wings 1, 2 and 3, although slightly underestimating the effect of thickness taper on wing 2. Combined with the estimates of Ref. 2 for the spanwise variation of the supervelocity distribution at the maximum thickness line, a close estimate of the velocity distribution over the whole surface of wing 2 can be obtained.

5.7 For wings tapered both in plan and thickness, the theories of Ref. 2 and Ref. 3 both underestimate the rate at which the supervelocity at the maximum thickness line increases outboard of the centre-section.

LIST OF SYMBOLS

A	aspect ratio
F	$\frac{v_x(k)_{\text{biconvex}}}{v_x(k)_{\text{RAE 101}}}$
R	Reynolds number
V_o	free stream velocity
c	wing chord
c_o	wing root chord
s	wing semi-span
t_o	wing maximum thickness at c_o
v_x	chordwise supervelocity
Δv_x	increment of chordwise supervelocity
η	spanwise co-ordinate y/s
λ	planform taper ratio $= \frac{\text{tip chord}}{\text{root chord}}$
μ	$\frac{\text{tip thickness/chord ratio}}{t_o/c_o}$
ϕ	angle of sweep

subscripts

x	chordwise direction
y	spanwise direction
k	maximum thickness position

LIST OF REFERENCES

No.	Author	Title, etc.
1	Peckham, D.H.	The geometry of wing surfaces generated by straight lines and with a high rate of thickness taper at the root. A.R.C. C.P.383. May, 1957.
2	Newby, K.W.	The effects of taper on the supervelocities on three dimensional wings at zero incidence. A.R.C. R. & M. 3032. June, 1955.
3	Neumark, S. and Collingbourne, J.	Velocity distribution on thin tapered wings with fore-and-aft symmetry and spanwise constant thickness ratio at zero incidence. A.R.C. R. & M. 2858. June, 1951.
4	Weber, J.	The calculation of the pressure distribution on thick wings of small aspect ratio at zero lift in subsonic flow. A.R.C. R. & M. 2993. September, 1954.
5	Peckham, D.H.	Low speed wind tunnel tests on a series of uncambered slender pointed wings with sharp edges. A.R.C. R. & M. 3186. December, 1958.
6	Kuchemann, D. Weber, J. and Brebner, G.G.	Low speed tests on 45-deg. swept-back wings. A.R.C. R. & M. 2882. May, 1951.

TABLE 1

Coefficients of pressure, C_p, at $\alpha = 0^\circ$

Wing 1

$\frac{x}{c}$	η				
	0	0.1	0.3	0.5	0.9
0	1.005	1.005	1.006	1.008	1.001
0.01	0.161	–	–	–	–
0.03	-0.149	–	–	-0.118	-0.161
0.05	-0.240	-0.233	-0.237	-0.199	-0.208
0.08	-0.300	–	–	–	–
0.13	-0.333	-0.327	-0.326	-0.313	-0.246
0.20	-0.346	-0.342	-0.341	-0.330	-0.246
0.25	-0.347	–	–	–	–
0.30	-0.350	-0.350	-0.348	-0.337	-0.250
0.35	-0.314	–	–	–	–
0.40	-0.274	-0.266	-0.268	-0.250	-0.210
0.50	-0.190	-0.190	-0.181	-0.177	-0.218
0.60	-0.122	-0.117	-0.111	-0.098	-0.090
0.75	-0.015	-0.024	-0.023	-0.013	-0.015
0.90	0.063	–	–	–	–

Wing 2

$\frac{x}{c}$	η			
	0	0.1	0.3	0.5
0	1.006	1.005	1.003	–
0.01	0.148	–	–	–
0.03	-0.123	–	–	–
0.05	-0.197	-0.198	-0.188	-0.138
0.08	-0.246	–	–	–
0.13	-0.267	-0.248	-0.215	-0.150
0.20	-0.271	-0.256	-0.218	-0.155
0.25	-0.263	–	–	–
0.30	-0.256	-0.241	-0.201	-0.153
0.35	-0.220	–	–	–
0.40	-0.190	-0.190	-0.161	-0.114
0.50	-0.131	-0.117	-0.108	-0.079
0.60	-0.086	-0.079	-0.062	-0.041
0.75	0.004	-0.005	-0.001	-0.001
0.90	0.070	–	–	–

TABLE 1 (CONTD)

Wing 3

x/c	η									
	0	0.1	0.2	0.3	0.4	0.5	0.6	0.7	0.8	0.9
0	1.006	0.549	0.509	0.495	0.487	0.482	0.481	0.470	0.461	0.422
0.01	0.495	0.206	0.167	0.139	0.125	0.130	0.112	0.119	0.110	0.068
0.03	0.212	0.023	-0.026	-0.055	-0.074	-0.076	-0.084	-0.088	-0.107	-0.138
0.05	0.110	-0.051	-0.101	-0.133	-0.147	-0.153	-0.161	-0.160	-0.183	-0.212
0.08	0.009	-0.111	-0.161	-0.192	-0.205	-0.210	-0.217	-0.221	-0.236	-0.253
0.13	-0.078	-0.161	-0.207	-0.232	-0.245	-0.249	-0.254	-0.255	-0.264	-0.254
0.20	-0.153	-0.217	-0.246	-0.264	-0.272	-0.273	-0.276	-0.274	-0.268	-0.234
0.25	-0.197	-0.244	-0.268	-0.278	-0.283	-0.284	-0.280	-0.271	-0.257	-0.219
0.30	-0.237	-0.262	-0.278	-0.286	-0.287	-0.281	-0.278	-0.265	-0.242	-0.205
0.35	-0.243	-0.259	-0.264	-0.267	-0.263	-0.259	-0.251	-0.234	-0.205	-0.170
0.40	-0.245	-0.240	-0.242	-0.240	-0.235	-0.226	-0.214	-0.181	-0.147	-0.137
0.50	-0.214	-0.204	-0.180	-0.165	-0.157	-0.147	-0.135	-0.157	-0.103	-0.081
0.60	-0.173	-0.138	-0.120	-0.113	-0.100	-0.087	-0.079	-0.060	-0.045	-0.034
0.75	-0.092	-0.065	-0.043	-0.024	-0.013	-0.004	0.008	0.018	0.026	0.026
0.90	-0.013	0.028	0.049	0.060	0.066	0.071	0.078	0.079	0.080	0.071

TABLE 1 (CONTD)

Wing 4

x/c	η			
	0	0.1	0.3	0.5
0	1.008	0.527	0.450	-
0.01	0.448	-	-	-
0.03	0.184	-	-	-
0.05	0.074	-0.072	-0.146	-0.140
0.08	-0.016	-	-	-
0.13	-0.093	-0.156	-0.185	-0.155
0.20	-0.154	-0.187	-0.191	-0.149
0.25	-0.184	-	-	-
0.30	-0.206	-0.210	-0.182	-0.127
0.35	-0.210	-	-	-
0.40	-0.200	-0.183	-0.149	-0.097
0.50	-0.164	-0.143	-0.101	-0.056
0.60	-0.121	-0.094	-0.059	-0.034
0.75	-0.050	-0.027	0.002	0.015
0.90	0.029	-	-	-

Wing 5

x/c	η		
	0	0.1	0.3
0	1.007	0.857	0.817
0.01	0.338	-	-
0.03	0.041	-	-
0.05	-0.063	-0.169	-0.221
0.08	-0.163	-	-
0.13	-0.225	-0.257	-0.304
0.20	-0.265	-0.281	-0.323
0.25	-0.273	-	-
0.30	-0.273	-0.286	-0.325
0.35	-0.245	-	-
0.40	-0.203	-0.219	-0.252
0.50	-0.116	-0.128	-0.163
0.60	-0.041	-0.061	-0.092
0.75	0.040	0.026	-0.002
0.90	0.116	-	-

Wing 6

x/c	η		
	0	0.1	0.3
0	0.994	0.350	0.271
0.01	0.495	-	-
0.03	0.224	-	-
0.05	0.118	-0.044	-0.125
0.08	0.030	-	-
0.13	-0.055	-0.143	-0.218
0.20	-0.119	-0.186	-0.250
0.25	-0.161	-	-
0.30	-0.196	-0.223	-0.260
0.35	-0.210	-	-
0.40	-0.207	-0.203	-0.217
0.50	-0.171	-0.162	-0.171
0.60	-0.115	-0.086	-0.088
0.75	-0.026	-0.012	-0.008
0.90	0.071	-	-

TABLE 1 (CONTD)

Wing 7

x/c	η		
	0	0.1	0.3
0	0.999	0.322	0.252
0.01	0.483	–	–
0.03	0.203	–	–
0.05	0.118	-0.056	-0.131
0.08	0.030	–	–
0.13	-0.053	-0.134	-0.166
0.20	-0.120	-0.163	-0.179
0.25	-0.142	–	–
0.30	-0.170	-0.190	-0.182
0.35	-0.173	–	–
0.40	-0.163	-0.162	-0.144
0.50	-0.133	-0.120	-0.107
0.60	-0.123	-0.077	-0.061
0.75	-0.015	-0.010	0.001
0.90	0.063	–	–

Wing 8

x/c	η		
	0	0.1	0.3
0	0.996	0.189	0.136
0.01	0.452	–	–
0.03	0.229	–	–
0.05	0.162	-0.028	-0.090
0.08	0.083	–	–
0.13	0.002	-0.102	-0.173
0.20	-0.050	-0.141	-0.201
0.25	-0.098	–	–
0.30	-0.127	-0.180	-0.220
0.35	-0.142	–	–
0.40	-0.154	-0.171	-0.187
0.50	-0.150	-0.145	-0.137
0.60	-0.132	-0.107	-0.085
0.75	-0.071	-0.042	-0.014
0.90	0.002	–	–

Wing A

x/c	η								
	0	0.1	0.2	0.3	0.4	0.5	0.6	0.7	0.8
0.01	0.358	–	–	–	–	–	–	–	–
0.03	0.253	0.374	0.128	0.163	0.052	0.134	–	–	–
0.05	0.192	0.146	0.123	0.108	0.095	0.087	0.071	0.064	–
0.08	0.120	0.082	0.059	0.046	0.031	0.017	–	–	–
0.13	0.029	-0.001	-0.023	-0.039	-0.058	-0.066	-0.069	-0.094	-0.107
0.20	-0.063	-0.091	-0.111	-0.125	-0.142	-0.151	–	–	–
0.25	-0.120	–	–	–	–	–	–	–	–
0.30	-0.164	-0.175	-0.190	-0.206	-0.222	-0.241	–	-0.268	-0.280
0.35	-0.196	–	–	–	–	–	–	–	–
0.40	-0.222	-0.229	-0.242	-0.255	-0.274	-0.294	-0.298	-0.321	-0.339
0.45	-0.239	–	–	–	–	–	–	–	–
0.50	-0.241	-0.248	-0.261	-0.274	-0.294	-0.307	-0.318	-0.343	-0.362
0.60	-0.223	-0.230	-0.244	-0.248	-0.278	-0.292	-0.299	-0.323	-0.340
0.70	-0.158	-0.171	-0.179	-0.195	-0.220	-0.232	-0.244	-0.267	-0.293
0.80	-0.022	-0.073	-0.092	-0.113	-0.131	-0.144	-0.153	-0.201	–
0.90	0.102	0.077	0.059	0.035	0.002	-0.007	-0.021	–	–
0.95	0.203	–	–	–	–	–	–	–	–

TABLE 1 (CONTD)

Wing B

$\frac{x}{c_o}$	η									
	0	0.1	0.2	0.3	0.4	0.5	0.6	0.7	0.8	0.9
0.10	0.101	0.097	0.093	0.091	0.094	0.090	0.098	0.093	0.096	0.107
0.20	0.044	0.042	0.040	0.044	0.046	0.043	0.049	0.052	0.060	0.062
0.30	-0.008	-0.011	-0.011	-0.003	0.010	-0.004	0.011	0.018	0.029	0.036
0.40	-0.055	-0.057	-0.059	-0.057	-0.050	-0.048	-0.038	-0.024	-0.010	0.007
0.50	-0.099	-0.102	-0.104	-0.103	-0.101	-0.097	-0.086	-0.070	-0.047	-0.023
0.60	-0.137	-0.141	-0.145	-0.144	-0.147	-0.144	-0.135	-0.120	-0.089	-0.055
0.70	-0.152	-0.158	-0.165	-0.170	-0.175	-0.181	-0.179	-0.168	-0.141	-0.094
0.80	-0.131	-0.135	-0.148	-0.154	-0.168	-0.185	-0.199	-0.202	-0.195	-0.148
0.90	-0.012	-0.024	-0.037	-0.050	-0.071	-0.100	-0.129	-0.165	-0.202	-0.211
0.95	0.100	0.087	0.076	0.065	0.048	0.019	-0.013	-0.062	-0.124	-0.206
0.98	-	0.192	0.175	0.170	0.162	0.149	0.132	0.206	0.046	-0.075

Note: $\eta = y/s(x)$ where $s(x)$ = local semi-span

TABLE 1 (CONTD)

Wing C

$\frac{x}{c_o}$	η									
	0	0.1	0.2	0.3	0.4	0.5	0.6	0.7	0.8	0.9
0.10	0.092	0.086	0.083	0.081	0.081	0.080	0.083	0.082	0.089	0.100
0.20	0.033	0.028	0.029	0.028	0.028	0.029	0.038	0.042	0.047	0.053
0.30	-0.004	-0.010	-0.007	-0.012	-0.011	-0.004	0.001	-0.002	0.012	0.021
0.40	-0.052	-0.055	-0.056	-0.055	-0.052	-0.048	-0.042	-0.036	-0.026	-0.011
0.50	-0.082	-0.081	-0.083	-0.084	-0.083	-0.080	-0.071	-0.066	-0.051	-0.039
0.60	-0.100	-0.103	-0.105	-0.111	-0.107	-0.108	-0.094	-0.090	-0.081	-0.058
0.70	-0.106	-0.108	-0.110	-0.113	-0.116	-0.120	-0.109	-0.106	-0.089	-0.070
0.80	-0.082	-0.084	-0.090	-0.099	-0.102	-0.103	-0.101	-0.102	-0.084	-0.070
0.90	-	0.002	-0.012	-0.025	-0.037	-0.046	-0.050	-0.040	-0.048	-0.046
0.95	-	0.094	0.073	0.056	0.035	0.017	0.004	-0.007	-0.016	-0.028
0.98	-	0.170	0.154	0.138	0.114	0.089	0.070	-	-	-

Note: $\eta = y/s(x)$ where $s(x)$ = local semi-span

TABLE 2

Coefficients of total lift, drag and pitching moment, from balance measurements, wings 1-8

Wings 1, 2, 3 and 4

$R = 3.2 \times 10^6$

Wing 1

α	$\overline{c}_L$	$\overline{c}_D$	$\overline{c}_m$
-1.43	-0.051	0.0085	-0.0025
-0.15	-0.003	0.0079	0.0004
1.13	0.046	0.0082	0.0023
2.56	0.095	0.0098	0.0049
3.84	0.147	0.0132	0.0070
5.12	0.197	0.0169	0.0093
6.50	0.249	0.0225	0.0101
7.89	0.303	0.0295	0.0109
9.22	0.361	0.0382	0.0104
10.56	0.418	0.0480	0.0092
11.90	0.478	0.0601	0.0082
13.23	0.539	0.0739	0.0063

Wing 2

α	$\overline{c}_L$	$\overline{c}_D$	$\overline{c}_m$
-2.48	-0.094	0.0081	-0.0037
-1.02	-0.036	0.0059	-0.0028
0.51	0.015	0.0056	-0.0001
1.94	0.069	0.0068	0.0020
3.43	0.128	0.0097	0.0029
4.82	0.191	0.0147	0.0030
6.56	0.259	0.0222	0.0041
9.54	0.398	0.0473	0.0036
12.78	0.539	0.0932	0.0035
13.86	0.588	0.1147	-0.0046

Wing 3

α	$\overline{c}_L$	$\overline{c}_D$	$\overline{c}_m$
-1.95	-0.079	0.0079	-0.0013
-0.82	-0.035	0.0062	0.0002
0.32	0.007	0.0059	0.0018
1.48	0.051	0.0065	0.0029
2.65	0.095	0.0085	0.0043
3.83	0.140	0.0109	0.0051
5.03	0.185	0.0146	0.0057
6.19	0.230	0.0192	0.0062
7.32	0.276	0.0252	0.0062
8.50	0.321	0.0316	0.0057
9.63	0.368	0.0388	0.0046
10.75	0.414	0.0473	0.0034
11.93	0.463	0.0572	0.0014
13.11	0.511	0.0681	-0.0013
14.25	0.560	0.0803	-0.0046
15.37	0.609	0.0938	-0.0088
16.51	0.659	0.1085	-0.0124
17.64	0.710	0.1243	-0.0196

Wing 4

α	$\overline{c}_L$	$\overline{c}_D$	$\overline{c}_m$
-3.18	-0.111	0.0087	-0.0050
-0.99	-0.030	0.0053	-0.0001
0	0.002	0.0051	0.0020
1.01	0.036	0.0056	0.0037
3.11	0.111	0.0093	0.0057
5.14	0.192	0.0168	0.0052
7.48	0.292	0.0310	0.0044
10.25	0.408	0.0546	0.0016
12.63	0.518	0.0843	-0.0022
14.79	0.625	0.1199	-0.0073
16.96	0.739	0.1683	-0.0156

TABLE 2 (CONTD)

Wings 5, 6, 7 and 8

R.N. = 2.1×10^6

Wing 5

α	$\bar{C}_L$	$\bar{C}_D$	$\bar{C}_m$
-4.46	-0.199	0.0140	-0.0101
-2.33	-0.104	0.0101	-0.0055
-0.30	-0.016	0.0088	-0.0015
0.71	0.029	0.0089	0.0006
1.71	0.072	0.0095	0.0028
3.71	0.161	0.0122	0.0071
5.72	0.248	0.0174	0.0109
7.75	0.333	0.0247	0.0149
10.77	0.455	0.0419	0.0197
12.80	0.533	0.0602	0.0209
14.82	0.592	0.0921	0.0167
16.83	0.631	0.1400	-0.0037

Wing 6

α	$\bar{C}_L$	$\bar{C}_D$	$\bar{C}_m$
-5.01	-0.237	0.0143	0.0246
-3.00	-0.144	0.0093	0.0153
-1.00	-0.048	0.0067	0.0039
0	0	0.0064	-0.0012
1.01	0.049	0.0066	-0.0068
3.04	0.146	0.0090	-0.0182
5.07	0.243	0.0145	-0.0291
7.13	0.338	0.0236	-0.0393
10.20	0.480	0.0454	-0.0550
12.26	0.570	0.0687	-0.0632
14.30	0.656	0.1017	-0.0727
16.35	0.737	0.1480	-0.0822
18.39	0.807	0.1949	-0.1184
20.44	0.869	0.2545	-0.1361

Wing 7

α	$\bar{C}_L$	$\bar{C}_D$	$\bar{C}_m$
-2.33	-0.096	0.0135	0.0088
-1.31	-0.048	0.0121	0.0030
0	0.001	0.0116	-0.0026
0.81	0.050	0.0118	-0.0086
2.03	0.098	0.0131	-0.0143
3.86	0.198	0.0191	-0.0265
6.19	0.300	0.0304	-0.0386
8.12	0.400	0.0474	-0.0481
10.24	0.497	0.0703	-0.0587
12.27	0.589	0.0998	-0.0673
14.40	0.678	0.1359	-0.0768
16.52	0.762	0.1842	-0.0892
18.54	0.831	0.2401	-0.1003

Wing 8

α	$\bar{C}_L$	$\bar{C}_D$	$\bar{C}_m$
-4.73	-0.204	0.0135	0.0415
-3.04	-0.128	0.0098	0.0256
-1.01	-0.045	0.0079	0.0097
0	-0.003	0.0075	0.0010
1.01	0.041	0.0076	-0.0086
2.88	0.120	0.0094	-0.0222
4.71	0.200	0.0134	-0.0377
7.08	0.295	0.0216	-0.0519
10.12	0.415	0.0389	-0.0753
11.94	0.494	0.0552	-0.0905
13.84	0.576	0.0777	-0.1044
15.88	0.646	0.1047	-0.1086
17.90	0.717	0.1412	-0.1151
19.87	0.786	0.1827	-0.1214
21.89	0.857	0.2274	-0.1322

WT.2078.C.P.571.K3 - Printed in England

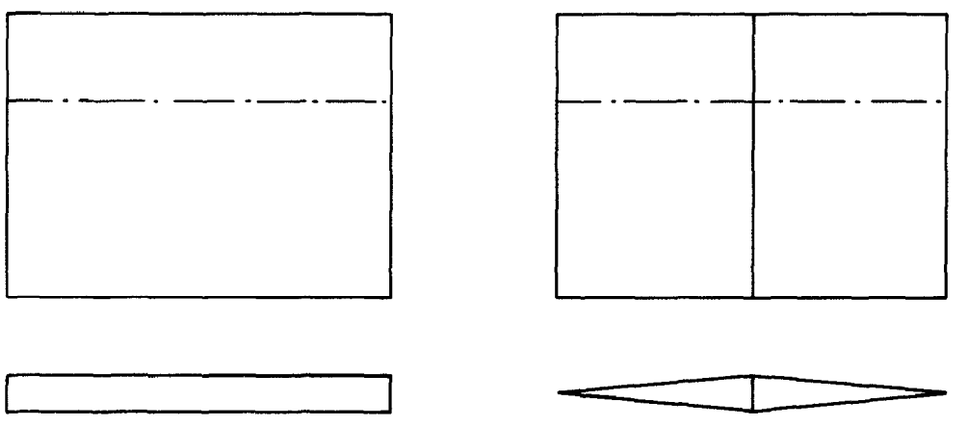

WING 1

WING 2

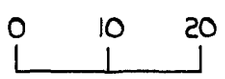

MODEL SCALE IN

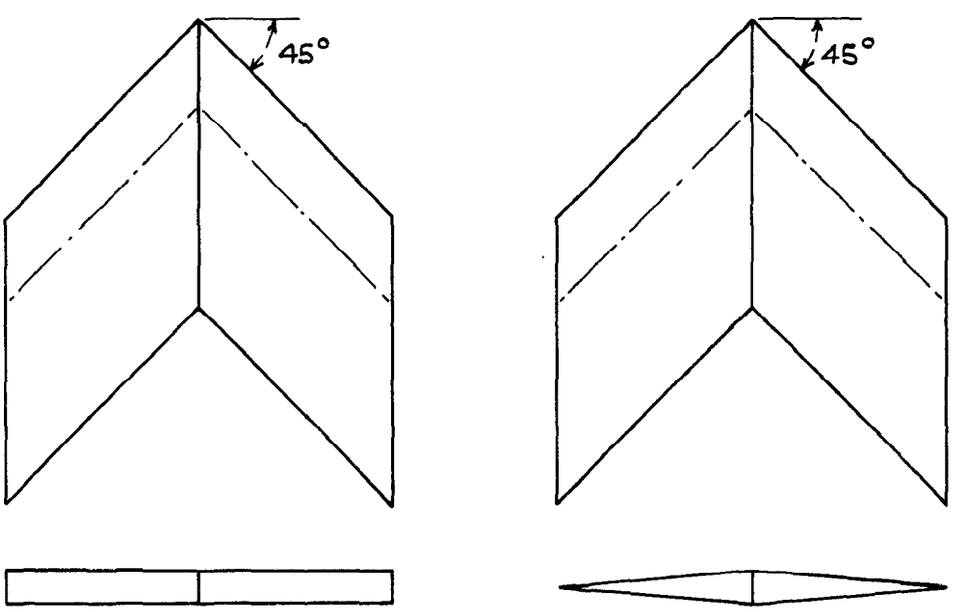

WING 3

WING 4

——·—— MAXIMUM THICKNESS POSITION

FIG. 1. CONSTANT CHORD WINGS.
ASPECT RATIO = 1·4.

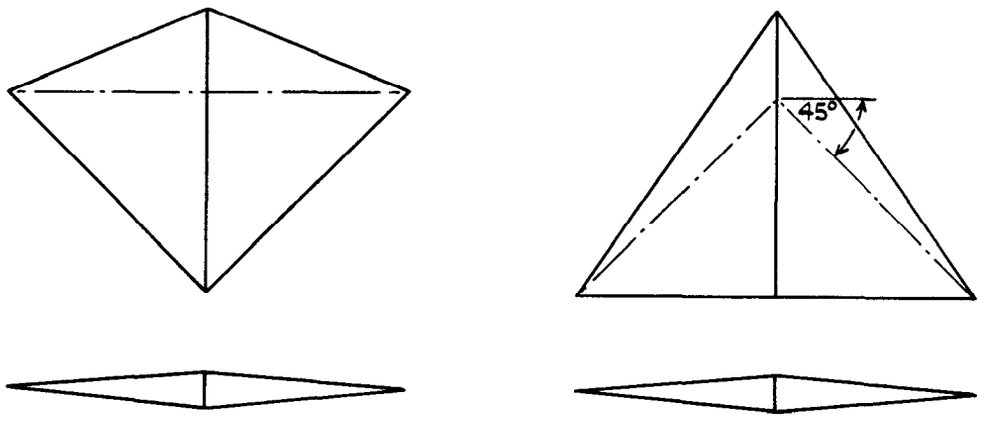

WING 5

WING 6

0 10 20

MODEL SCALE IN

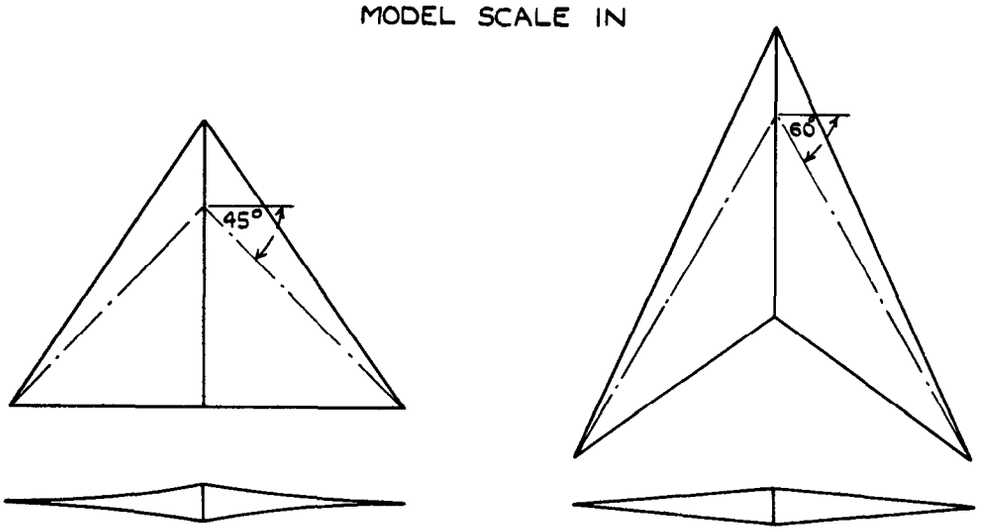

WING 7

WING 8

——·—— MAXIMUM THICKNESS POSITION

FIG. 2. WINGS OF PLANFORM TAPER RATIO 0 ASPECT RATIO = 2·8.

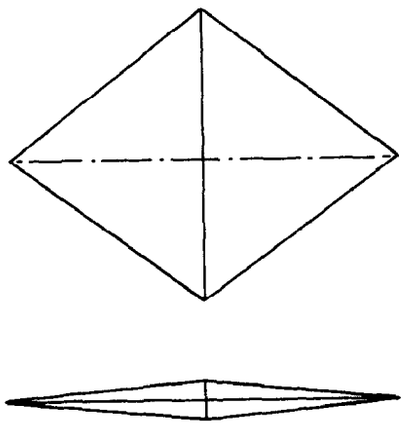

WING A

A = 2·8

0 10 20

MODEL SCALE IN

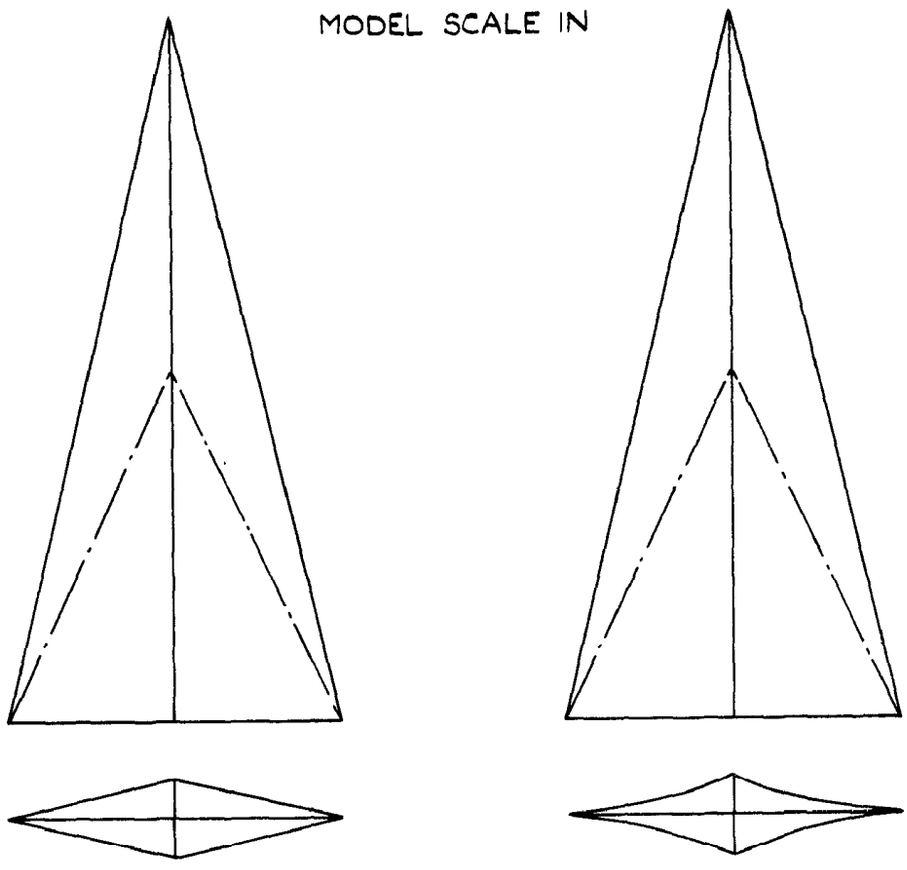

WING B

A = 1·0

WING C

A = 1·0

——·—— MAXIMUM THICKNESS POSITION

FIG. 3. WINGS OF BICONVEX PARABOLIC ARC SECTION

WINGS B & C — SEE REF. 5.

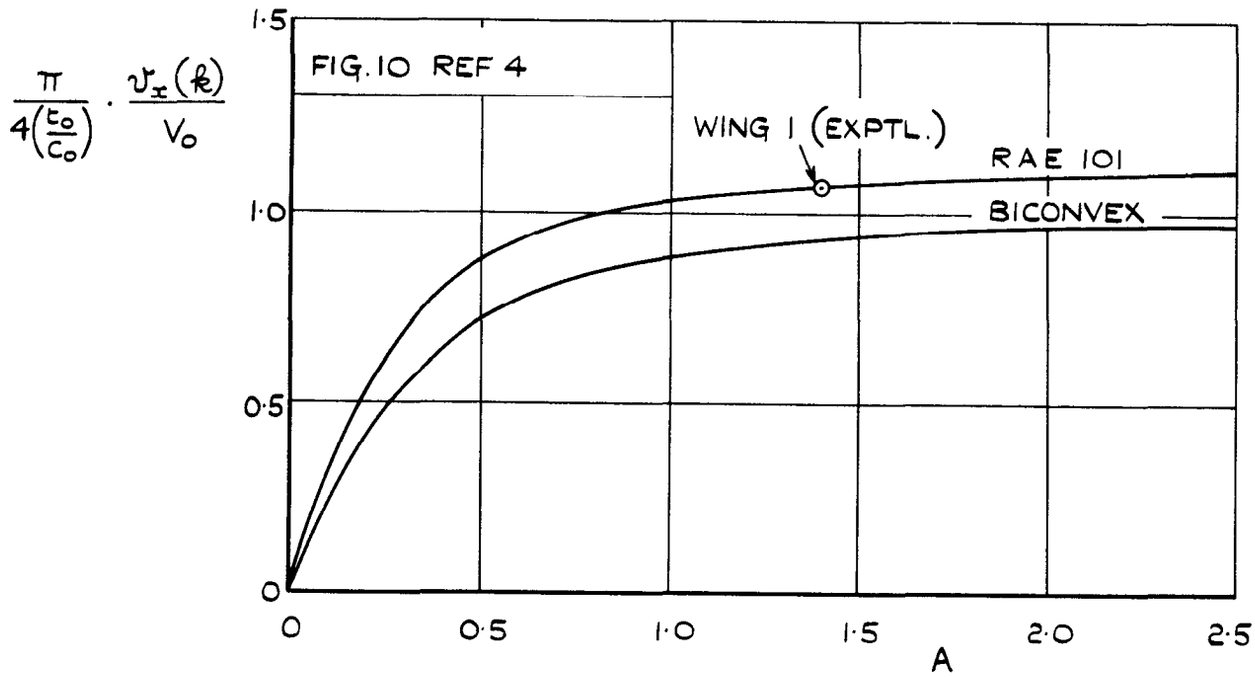

FIG. 4. EFFECT OF SECTION SHAPE ON SUPERVELOCITIES AT CENTRE SECTION OF RECTANGULAR WINGS $\alpha = 0°$ CONSTANT t/c

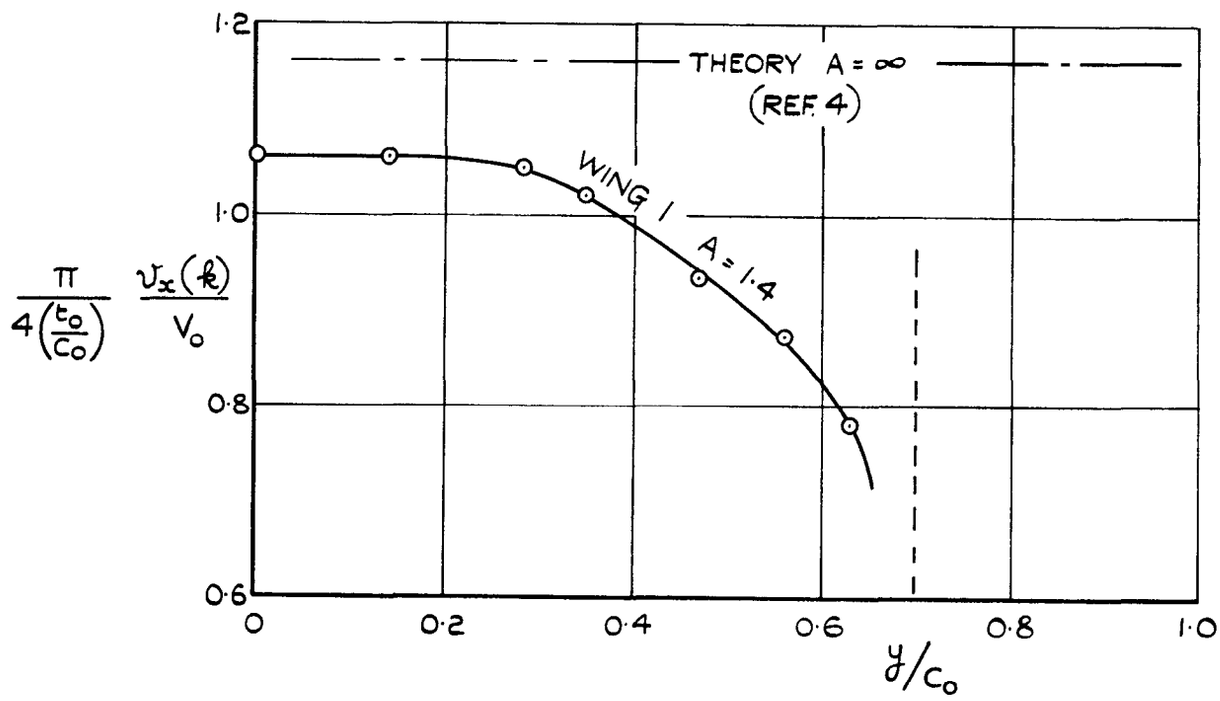

FIG. 5. EFFECT OF FINITE SPAN ON SUPERVELOCITIES AT t_{MAX} OF RECTANGULAR WING. $\alpha = 0°$ CONSTANT t/c

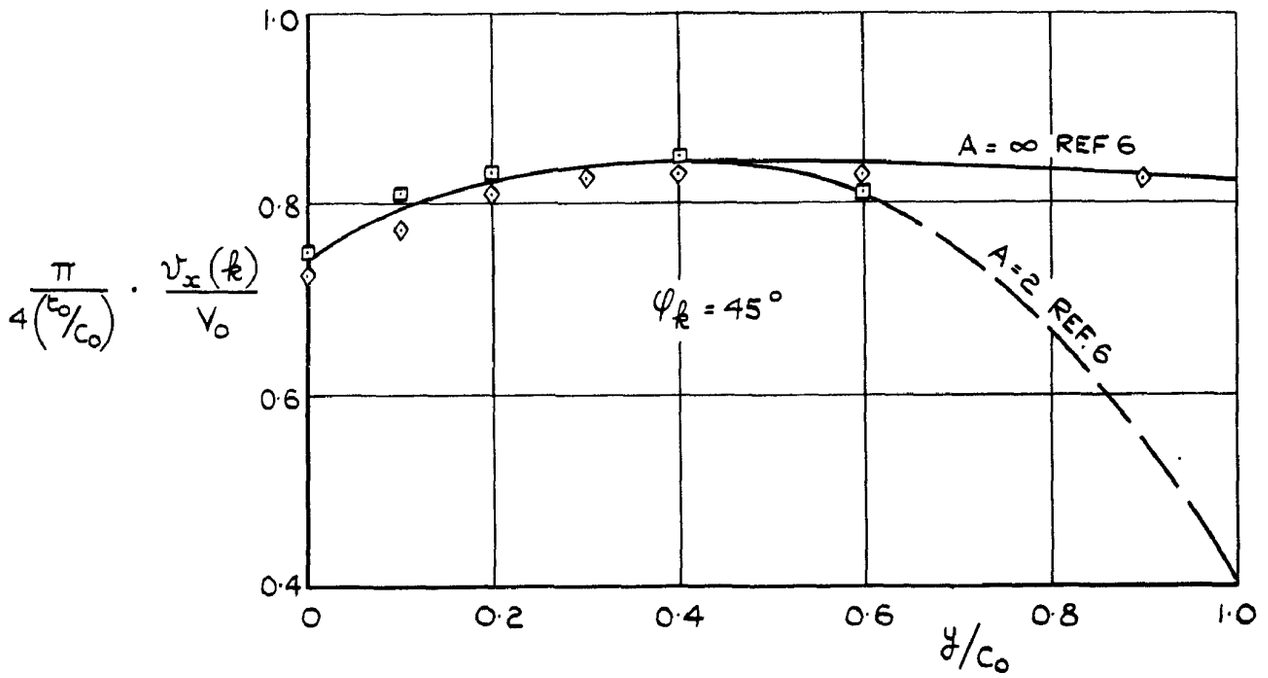

FIG. 6. EFFECT OF FINITE SPAN ON SUPERVELOCITIES AT t_{MAX} OF SWEPT CONSTANT-CHORD WINGS.
$\alpha = 0°$ CONSTANT t/c

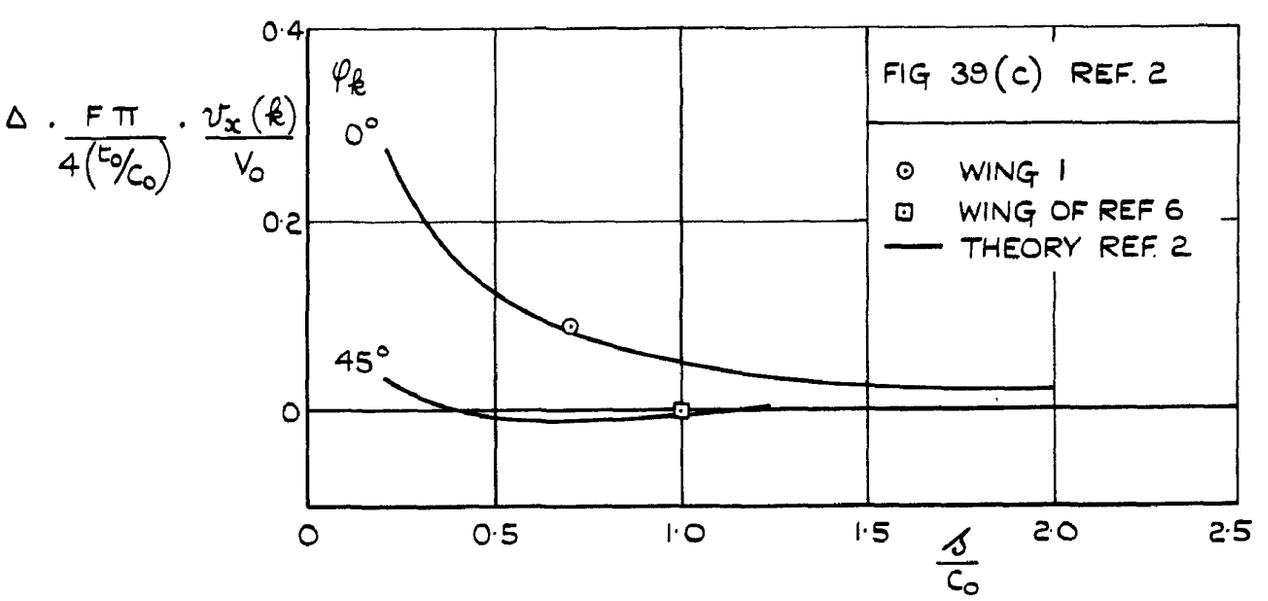

FIG. 7. EFFECT OF FINITE SPAN ON SUPERVELOCITY AT CENTRE-SECTION OF CONSTANT CHORD WINGS.
$\alpha = 0°$

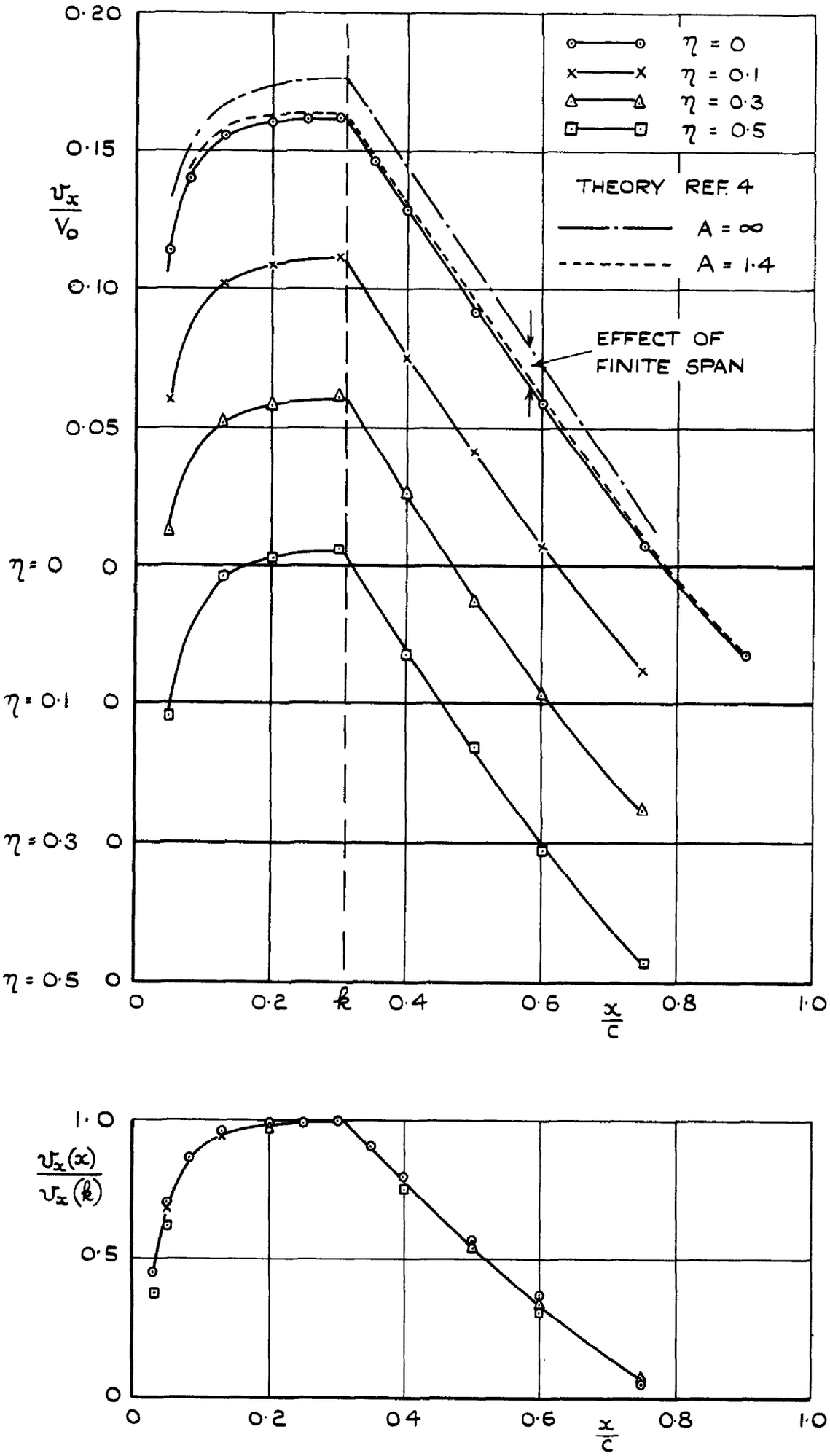

FIG. 8. WING 1. SUPERVELOCITIES AT $\alpha = 0°$

$A = 1·4 \quad \varphi_k = 0° \quad \mu = 1 \quad \frac{t_0}{c_0} = 0·12$

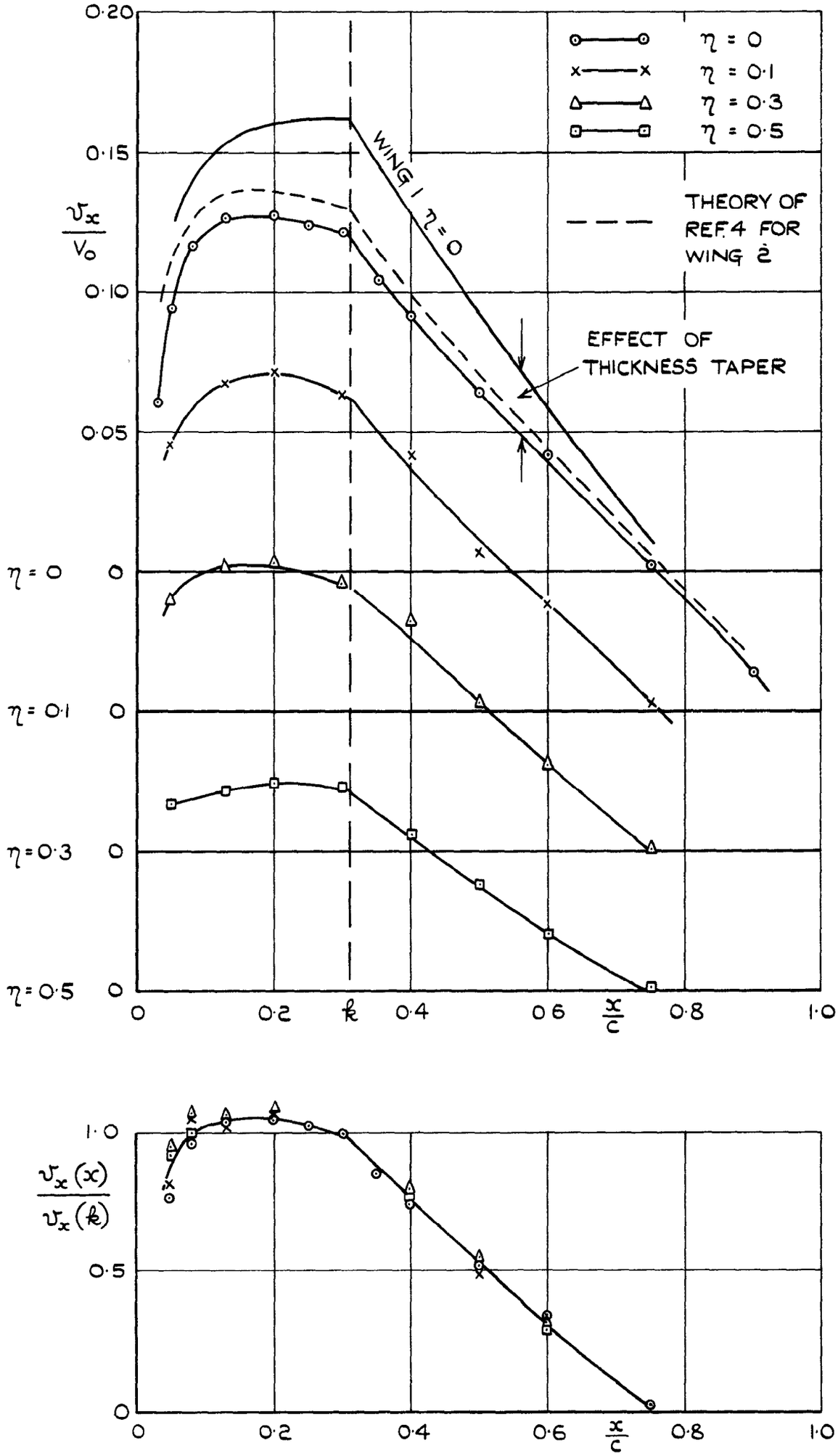

FIG. 9. WING 2. SUPERVELOCITIES AT $\alpha = 0°$

$A = 1·4 \quad \varphi_k = 0 \quad \mu = 0 \quad \frac{t_0}{c_0} = 0·12$

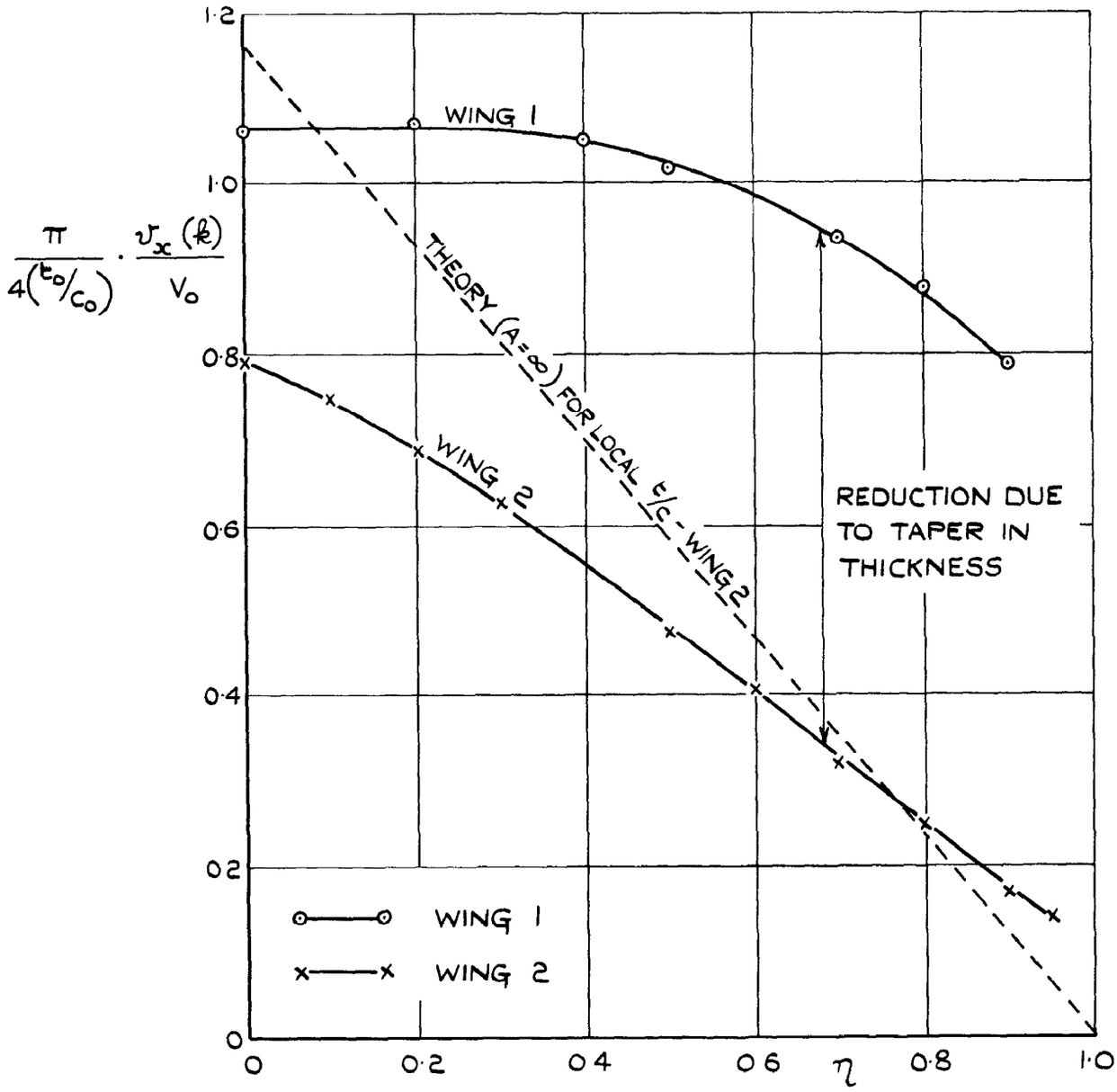

(a) EFFECT OF THICKNESS TAPER

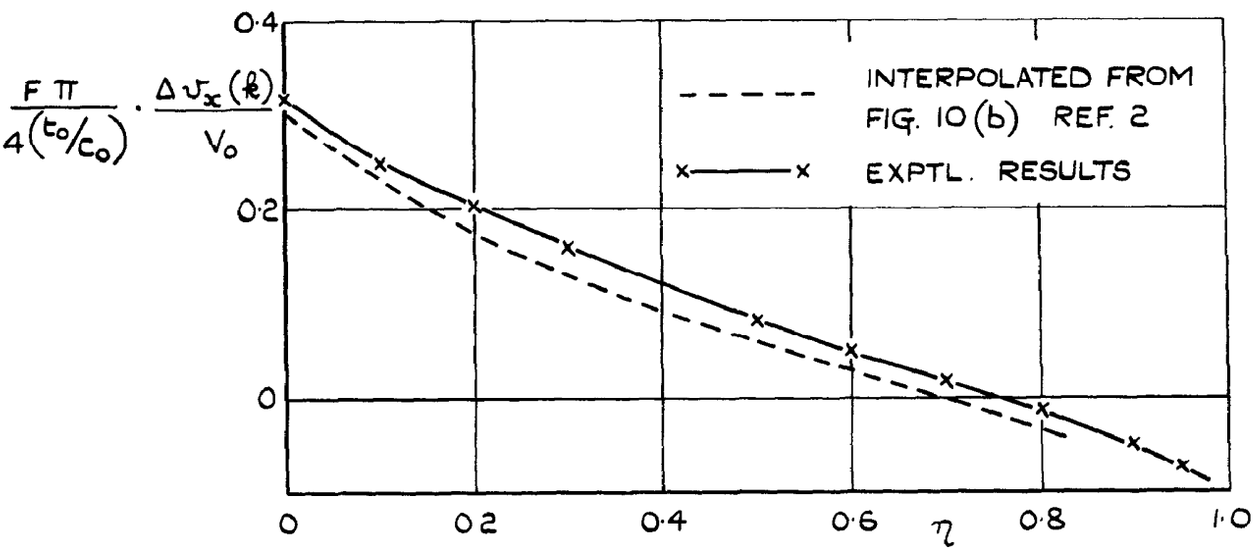

(b) REDUCTION OF v_x RELATIVE TO TWO-DIMENSIONAL VALUE FOR LOCAL THICKNESS/CHORD RATIO

FIG. 10 (a & b) SPANWISE VARIATION OF SUPERVELOCITY AT MAX. THICKNESS WINGS 1 & 2. $\alpha = 0^\circ$ $A = 1{\cdot}4$ $\varphi_k = 0^\circ$ $\frac{t_o}{c_o} = 0{\cdot}12$

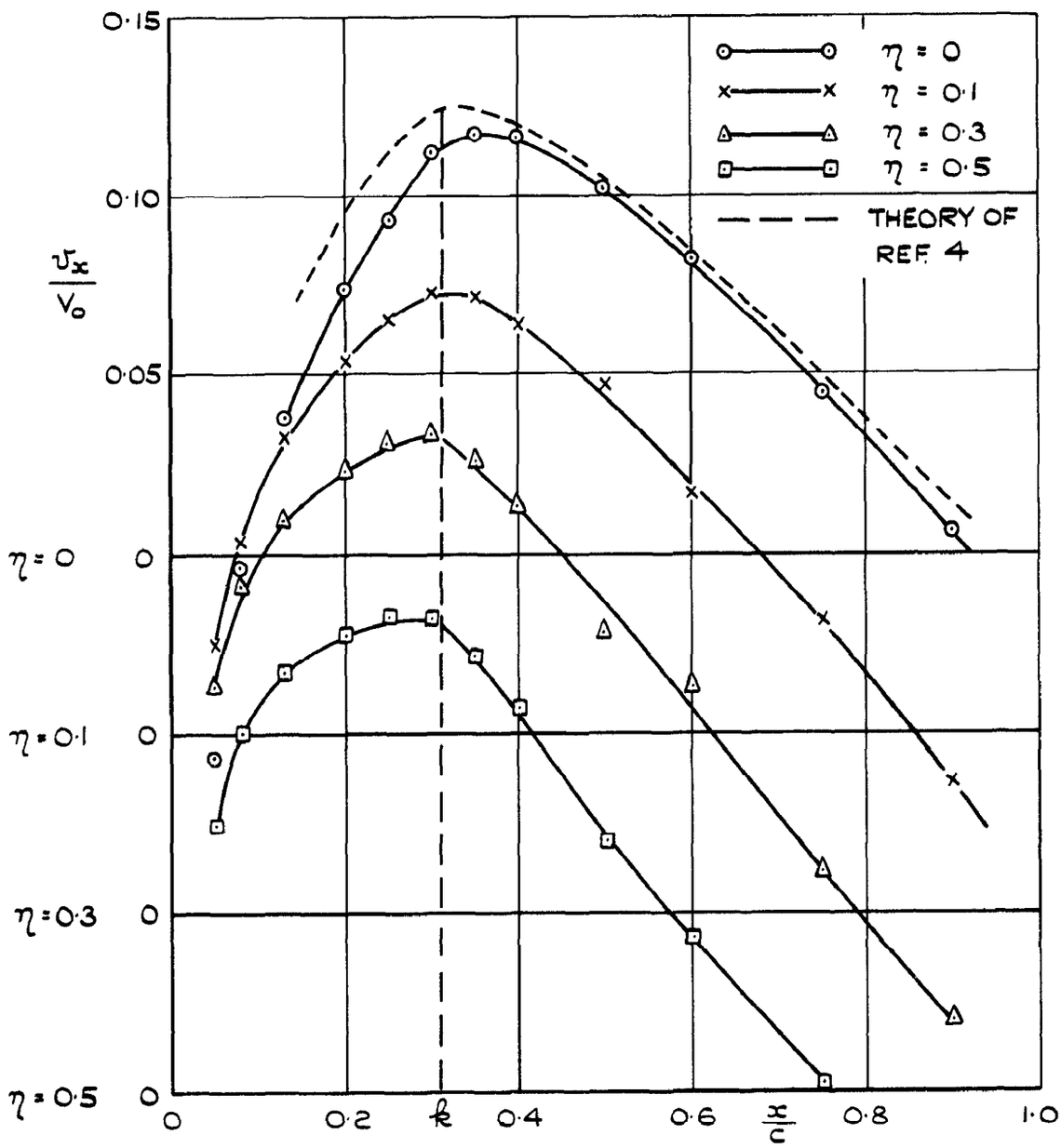

FIG.11. WING 3. SUPERVELOCITIES AT $\alpha = 0^\circ$

$A = 1{\cdot}4 \quad \varphi_k = 45^\circ \quad \mu = 1 \quad \frac{t_0}{c_0} = 0{\cdot}12$

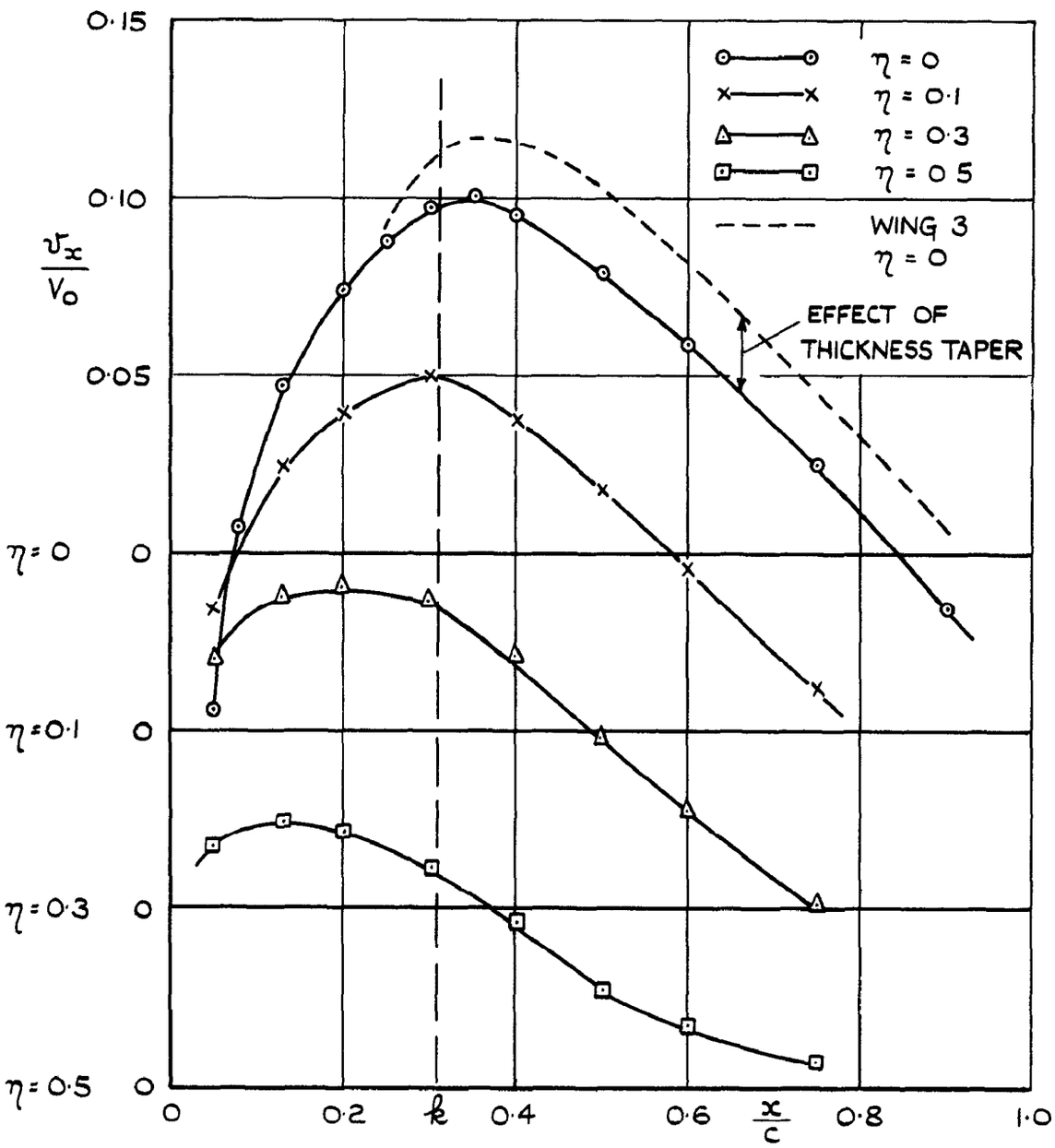

FIG. 12. WING 4. SUPERVELOCITIES AT $\alpha = 0^\circ$

$A = 1·4 \quad \varphi_k = 45^\circ \quad \mu = 0 \quad \frac{t_0}{c_0} = 0·12$

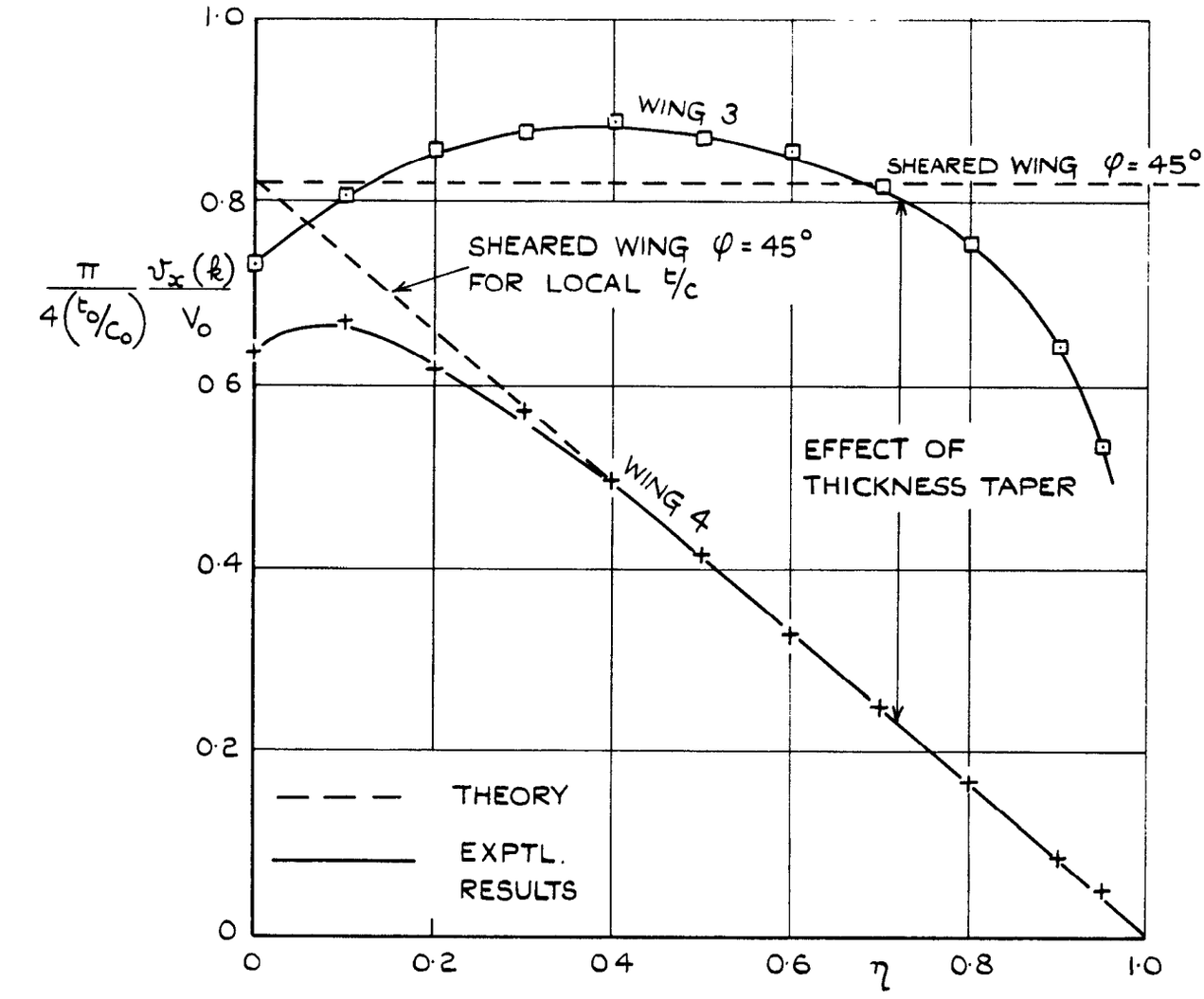

(a) EFFECT OF THICKNESS TAPER

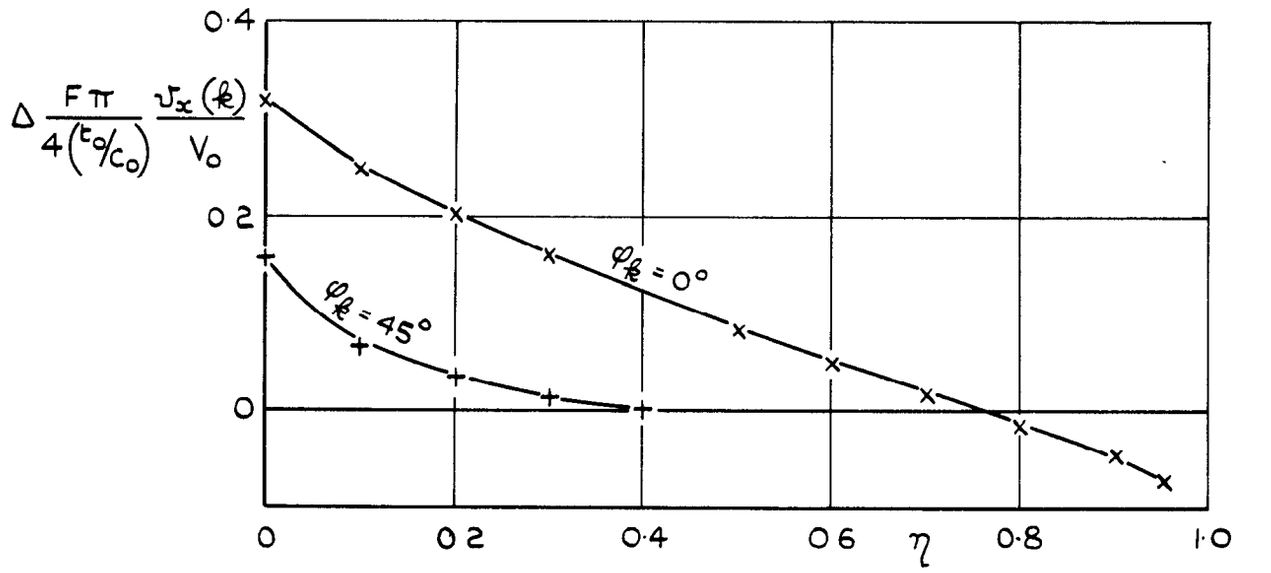

(b) REDUCTION OF v_x RELATIVE TO TWO-DIMENSIONAL VALUE FOR LOCAL THICKNESS/CHORD RATIO (SEE FIG. 10.)

FIG. 13 (a & b) SPANWISE VARIATION OF SUPERVELOCITY AT MAX. THICKNESS LINE. WINGS 3 & 4.

$\alpha = 0^\circ \quad A = 1 \cdot 4 \quad \varphi_k = 45^\circ \quad \frac{t_0}{c_0} = 0 \cdot 12$

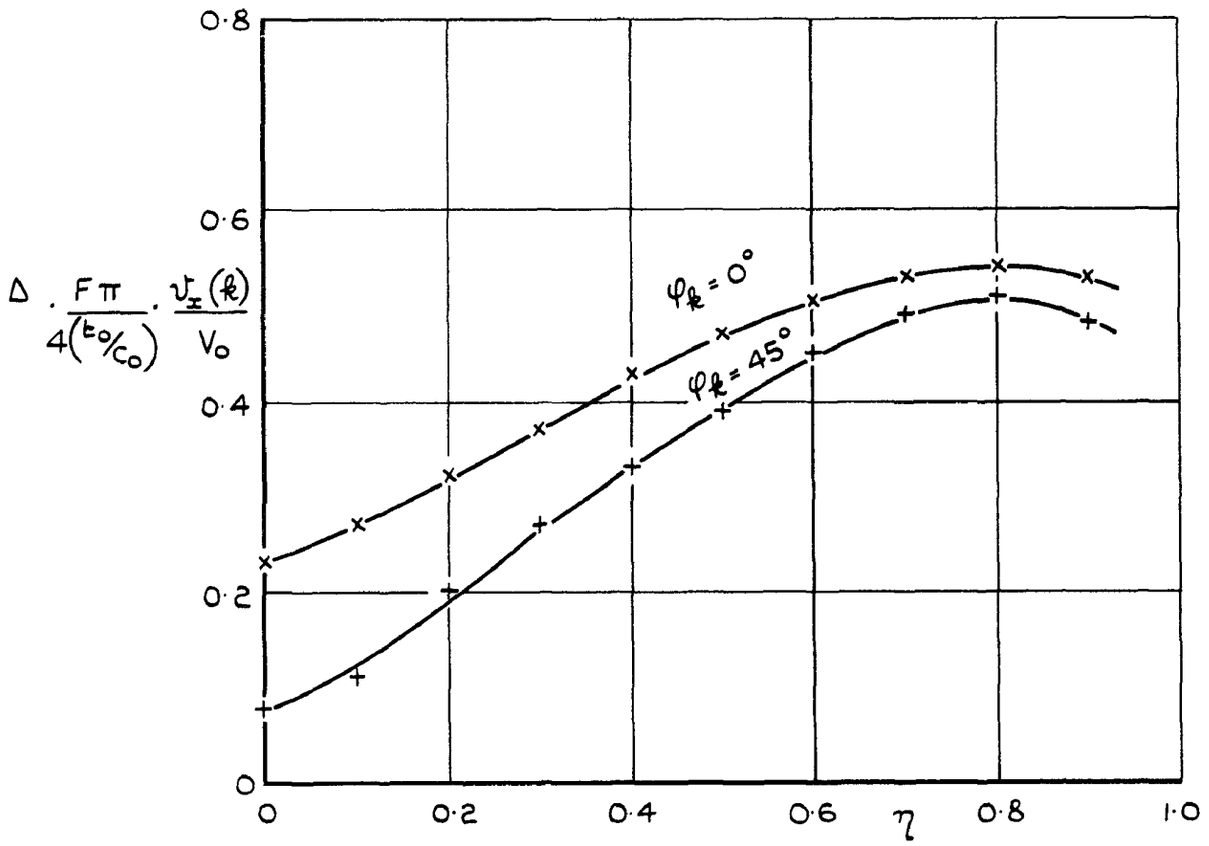

(a) REDUCTION OF SUPERVELOCITY AT MAXIMUM THICKNESS (EXPERIMENTAL)

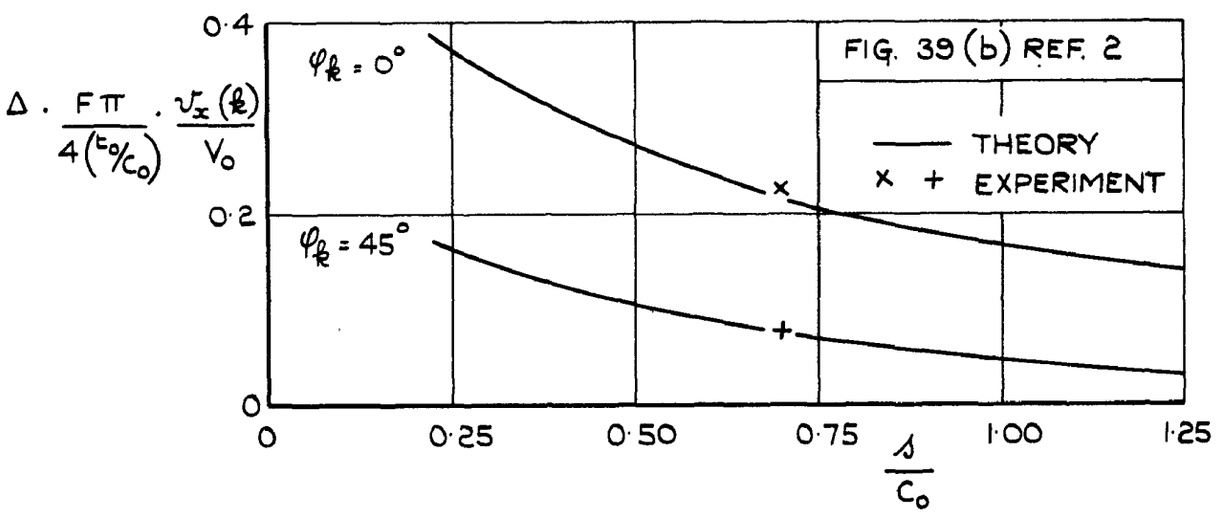

(b) REDUCTION OF SUPERVELOCITY AT MAXIMUM THICKNESS OF CENTRE-SECTION. COMPARISON WITH THEORY OF REF. 2.

FIG.14 (a & b) REDUCTION OF SUPERVELOCITY ON CONSTANT CHORD WINGS DUE TO THICKNESS TAPER

× DIFFERENCE BETWEEN WINGS 1 & 2
\+ DIFFERENCE BETWEEN WINGS 3 & 4
} A.R. = 1·4

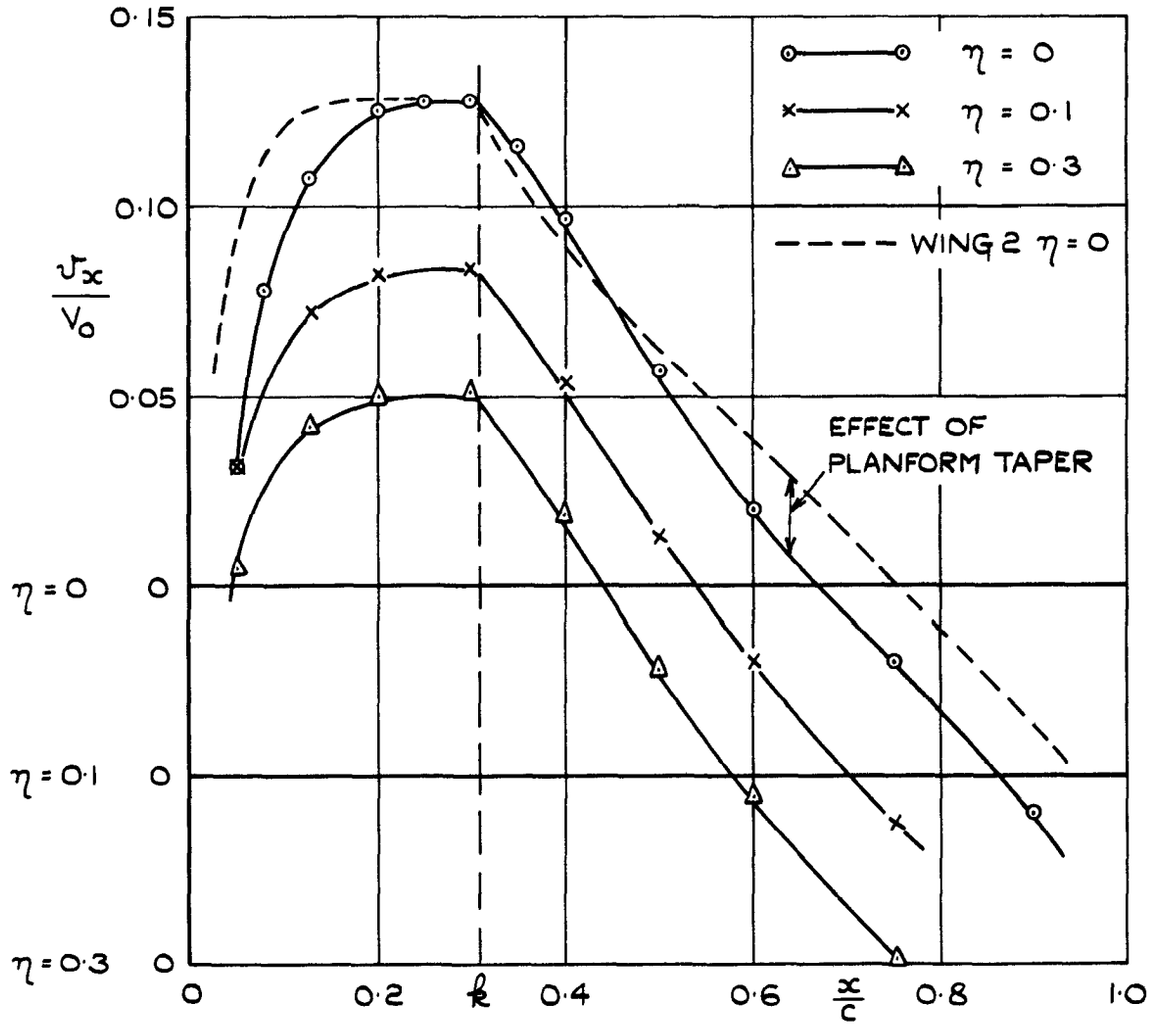

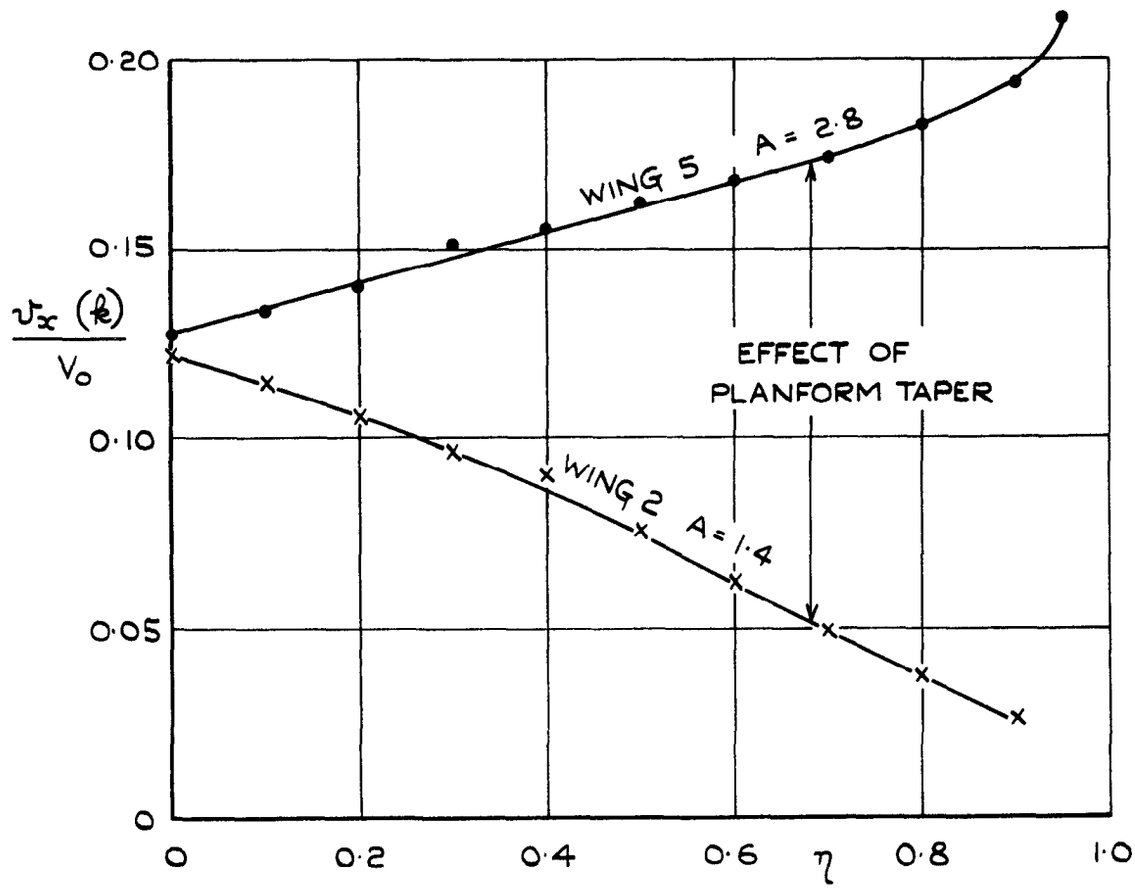

FIG.15. WING 5. SUPERVELOCITIES AT $\alpha = 0^\circ$

$A = 2{\cdot}8 \quad \varphi_k = 0 \quad \mu = 1 \quad \frac{t_0}{c_0} = 0{\cdot}12$

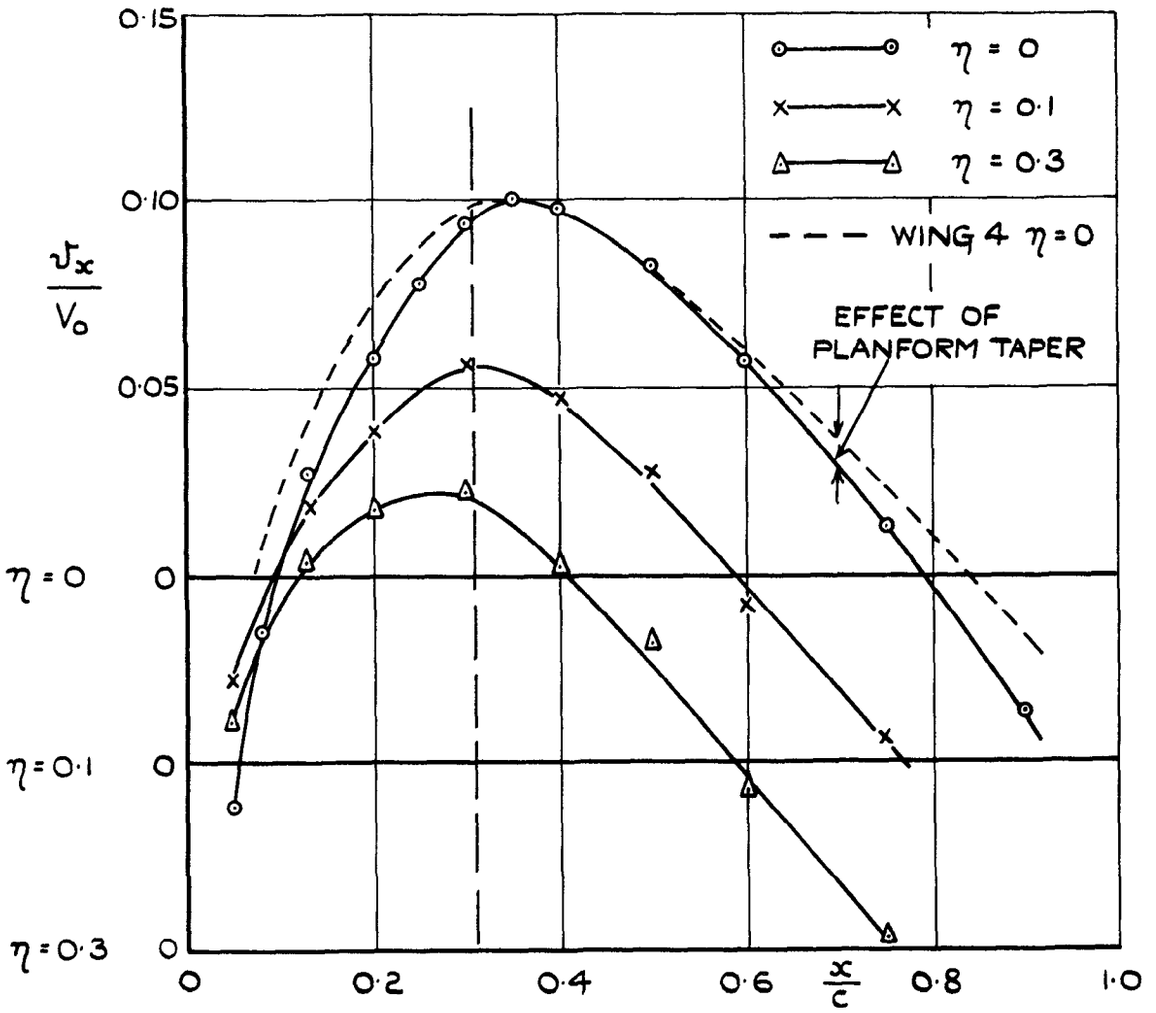

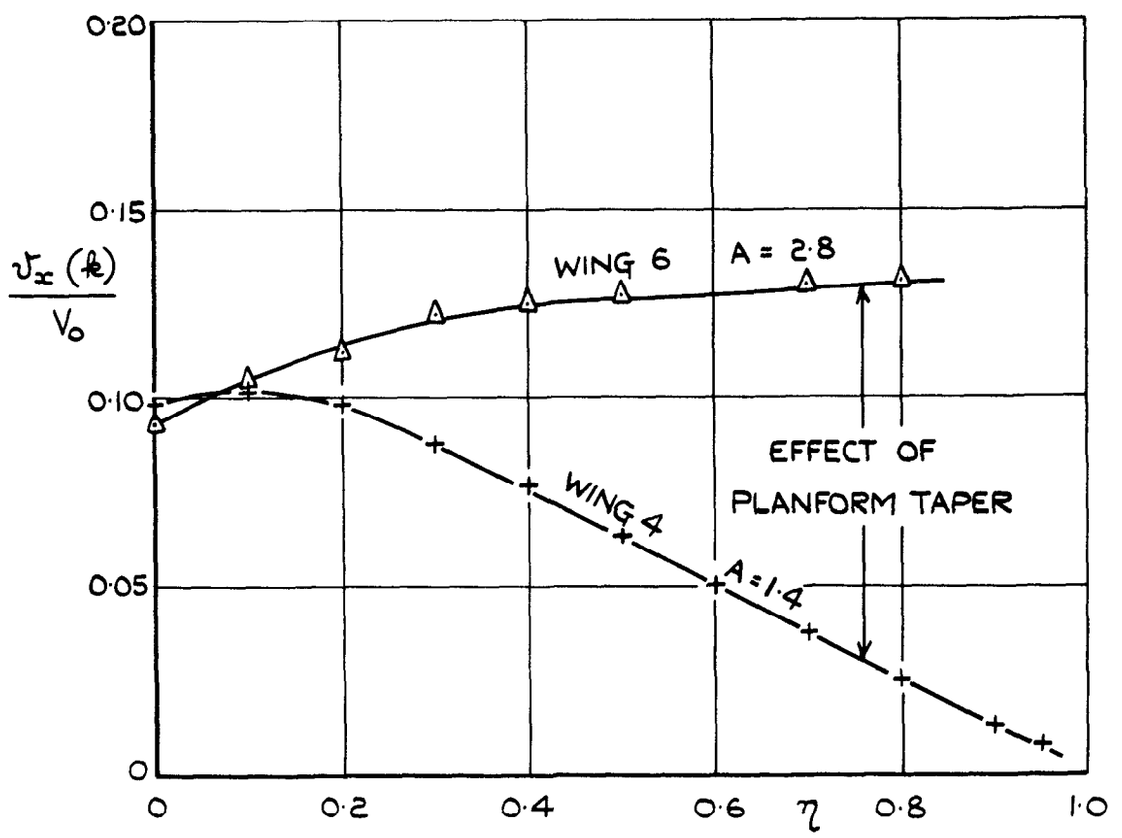

FIG. 16. WING 6. SUPERVELOCITIES AT $\alpha = 0^\circ$
$A = 2{\cdot}8 \quad \varphi_k = 45^\circ \quad \mu = 1 \quad \frac{t_0}{c_0} = 0{\cdot}12$

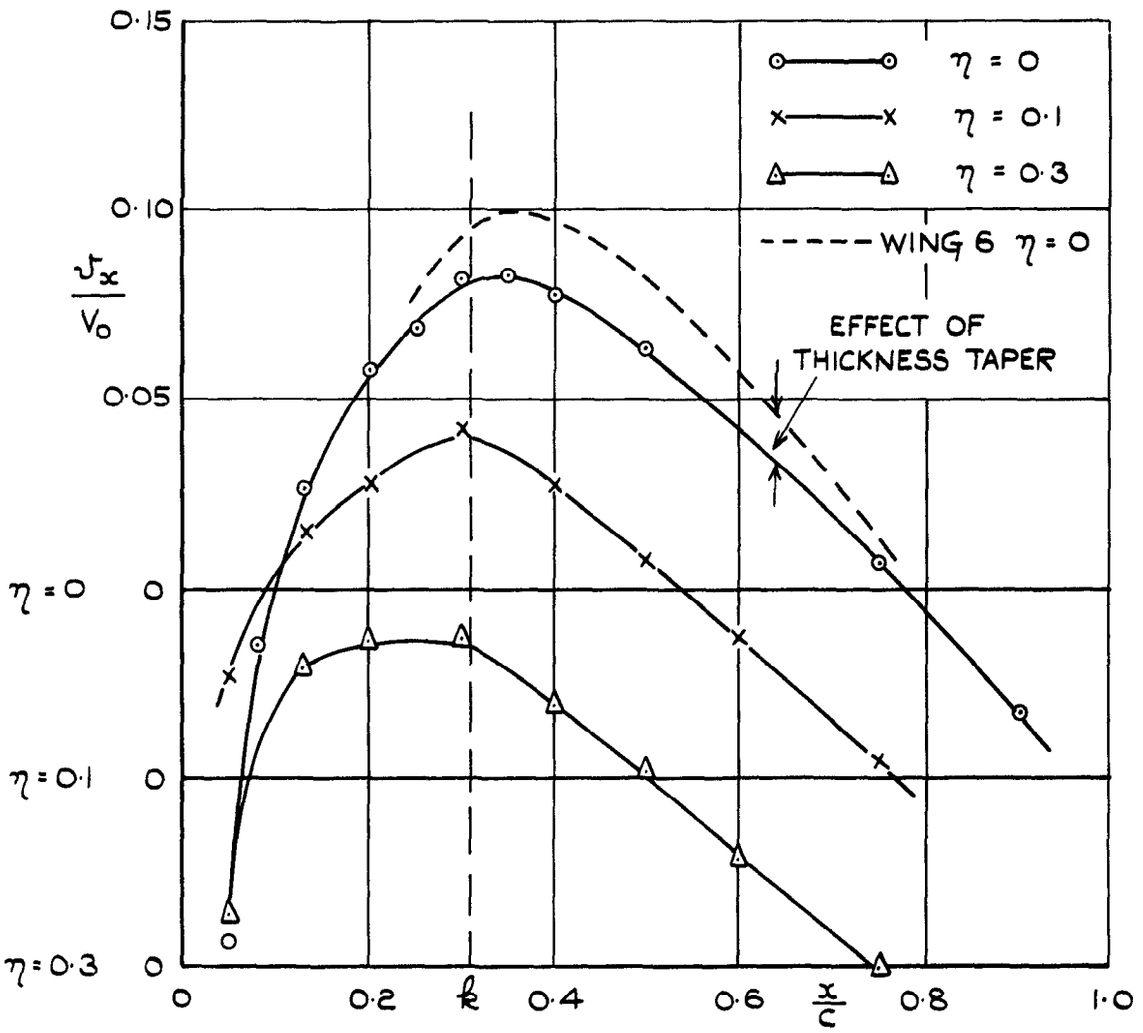

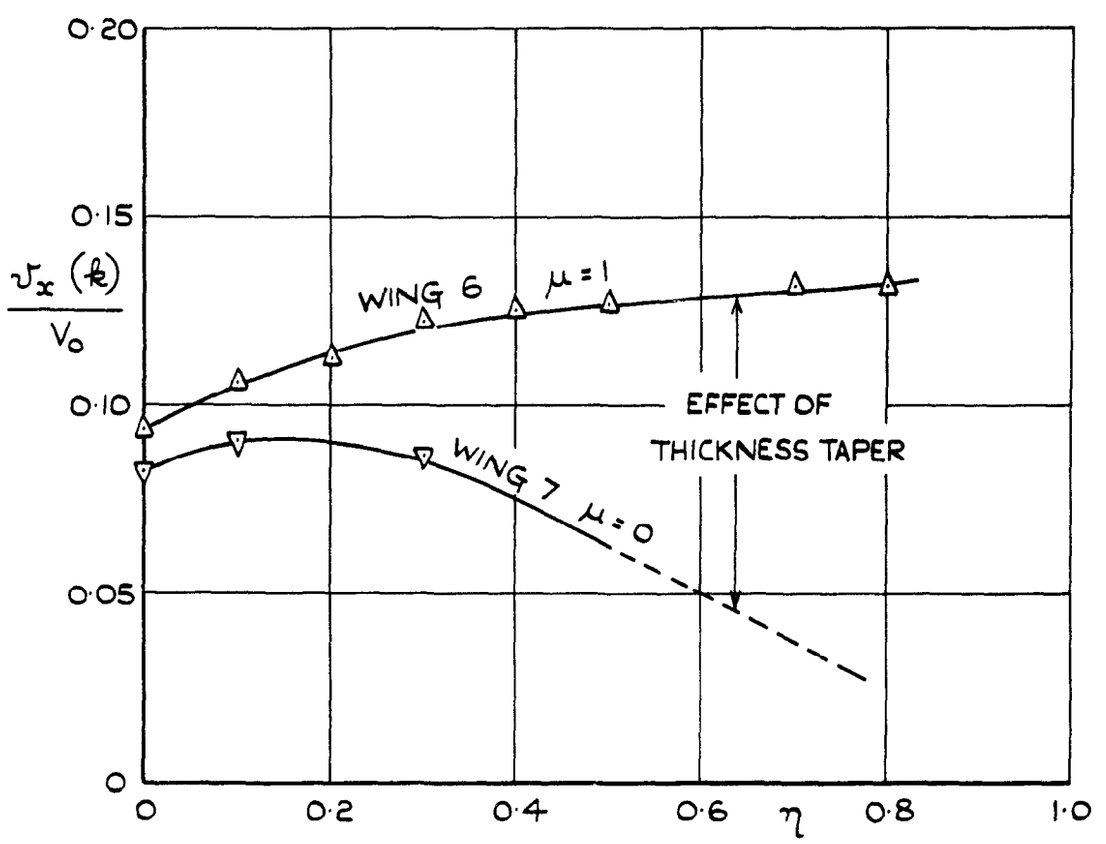

FIG.17. WING 7. SUPERVELOCITIES AT $\alpha = 0^\circ$
$A = 2{\cdot}8 \quad \varphi_k = 45^\circ \quad \mu = 0 \quad \frac{t_0}{c_0} = 0{\cdot}12$

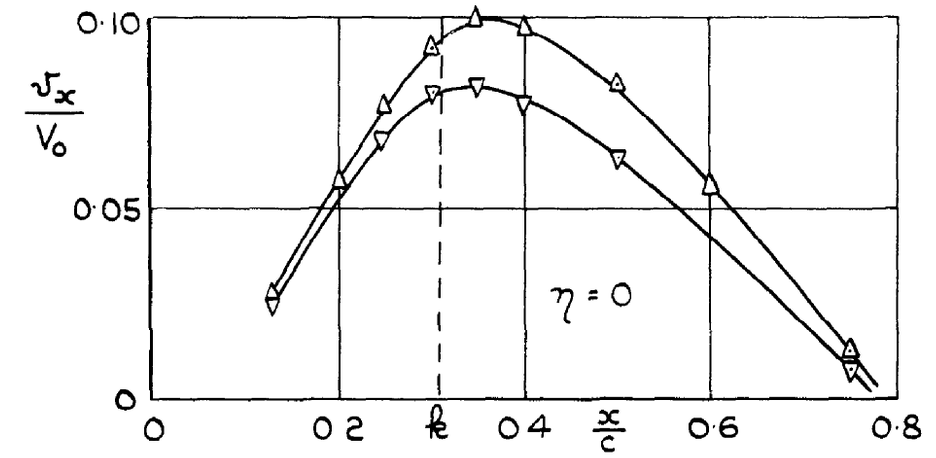

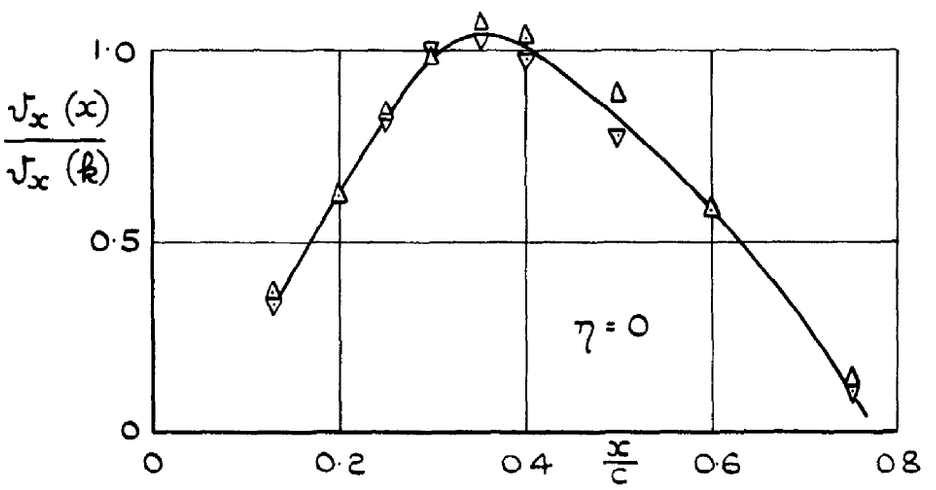

(a) CENTRE DISTRIBUTION

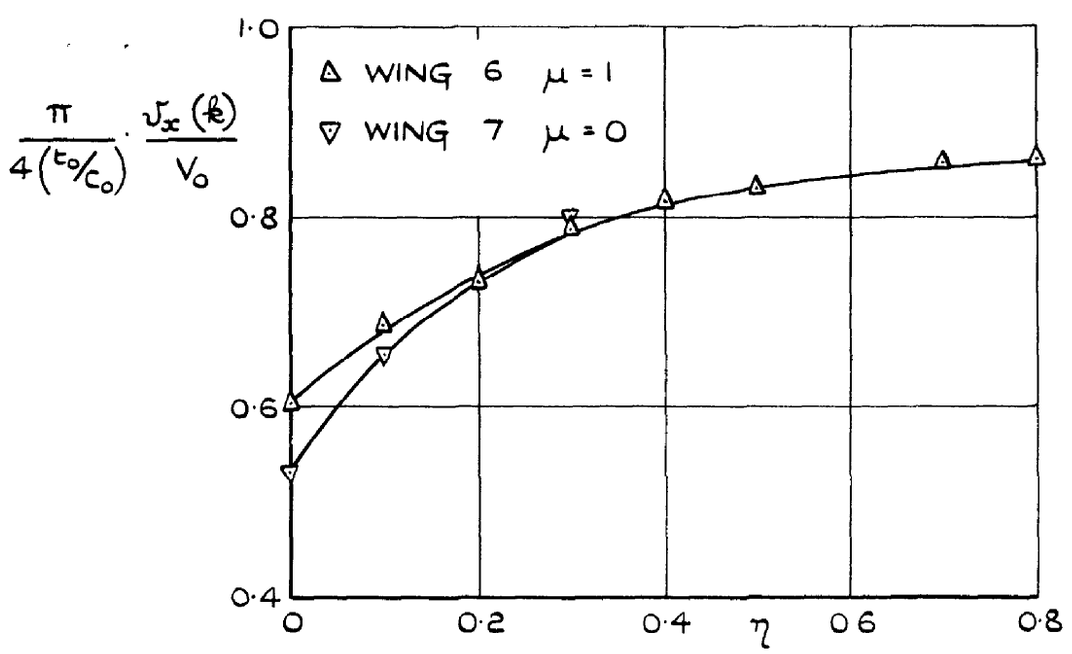

(b) MAX. THICKNESS DISTRIBUTION

FIG.18 (a & b) EFFECT OF DIFFERENT RATES OF THICKNESS TAPER ON WING TAPERED IN PLAN. WINGS 6 AND 7 $A = 2{\cdot}8$ $\varphi_{\frac{1}{4}} = 45^\circ$ $\alpha = 0^\circ$

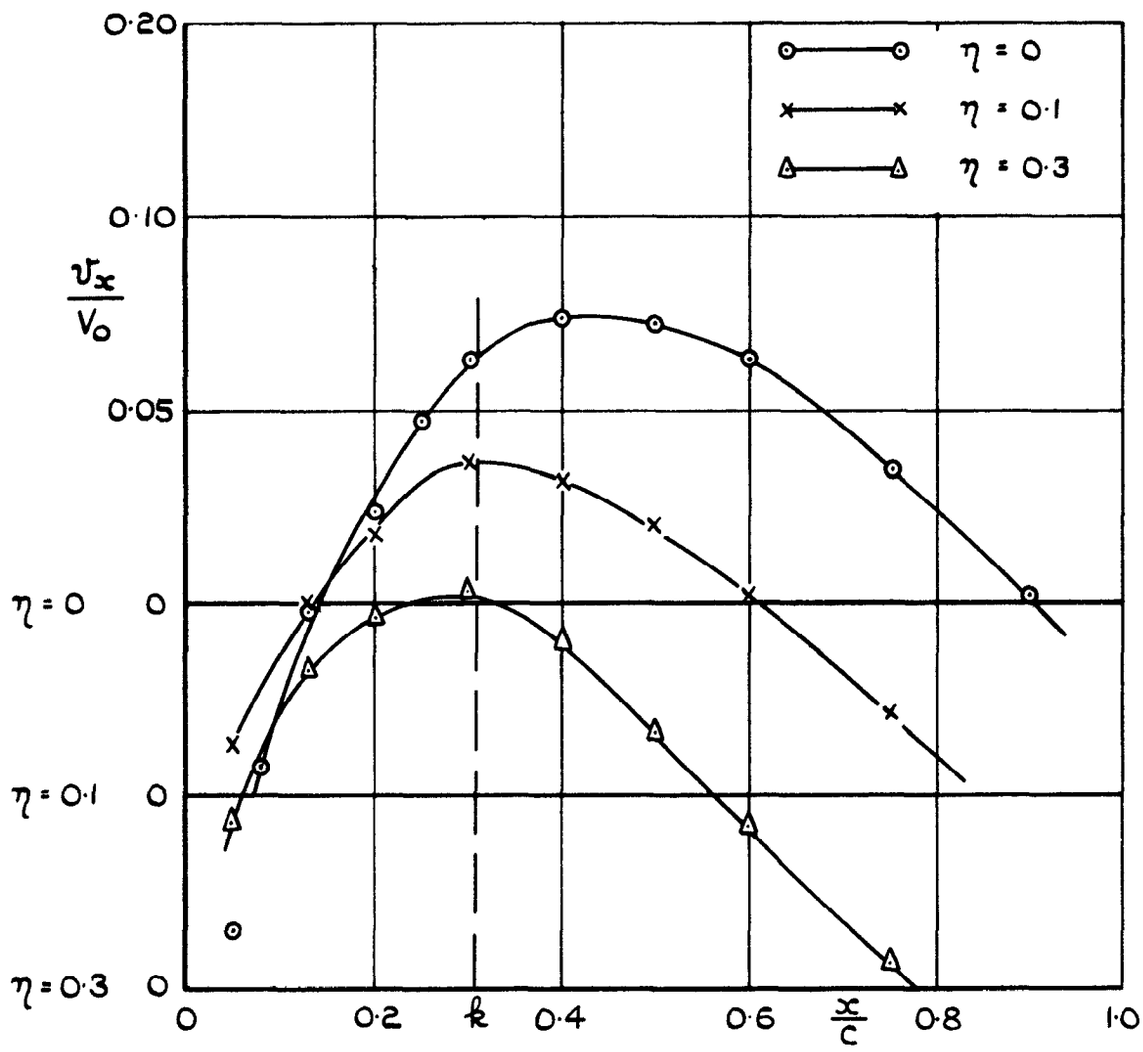

FIG. 19. WING 8. SUPERVELOCITIES AT $\alpha = 0^\circ$
$A = 2{\cdot}8 \quad \varphi_k = 60^\circ \quad \mu = 1 \quad \frac{t_0}{c_0} = 0{\cdot}12$

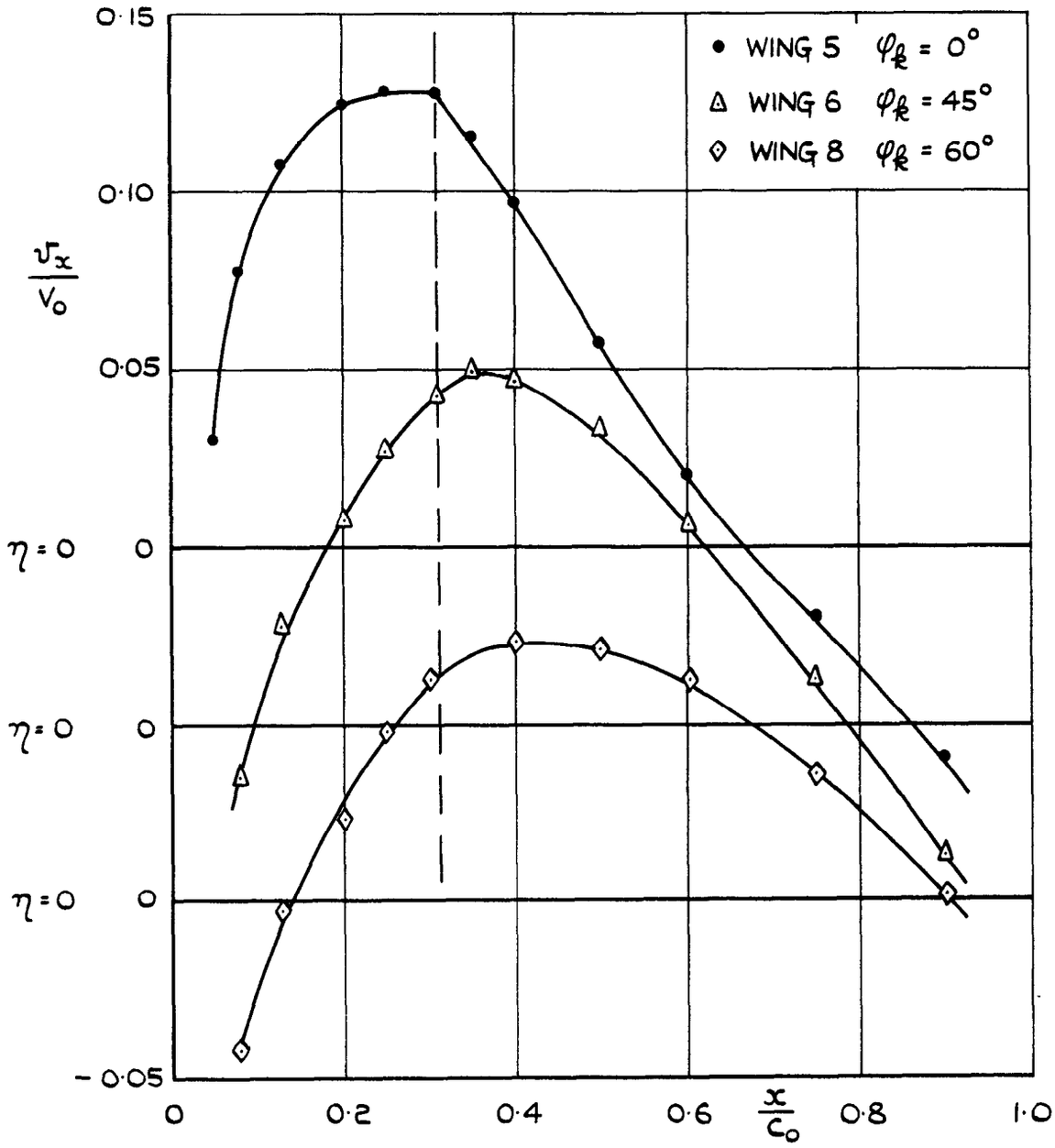

FIG. 20. WINGS 5, 6 & 8. EFFECT OF SWEEP ON CENTRE DISTRIBUTIONS. $\alpha = 0°$

$A = 2{\cdot}8 \quad \mu = 1 \quad \lambda = 0 \quad \frac{t_0}{c_0} = 0{\cdot}12$

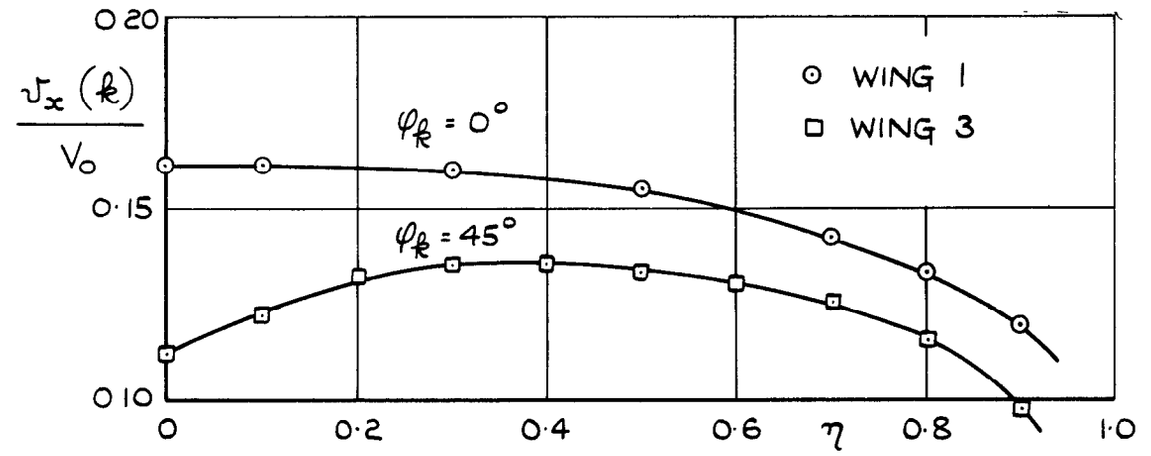

(a) A = 1·4 μ = 1 λ = 1

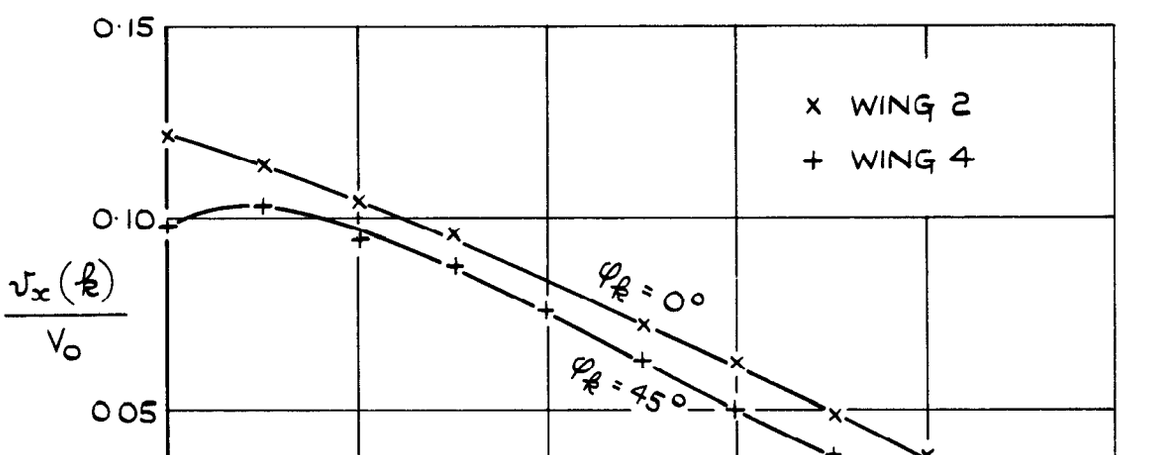

(b) A = 1·4 μ = 0 λ = 1

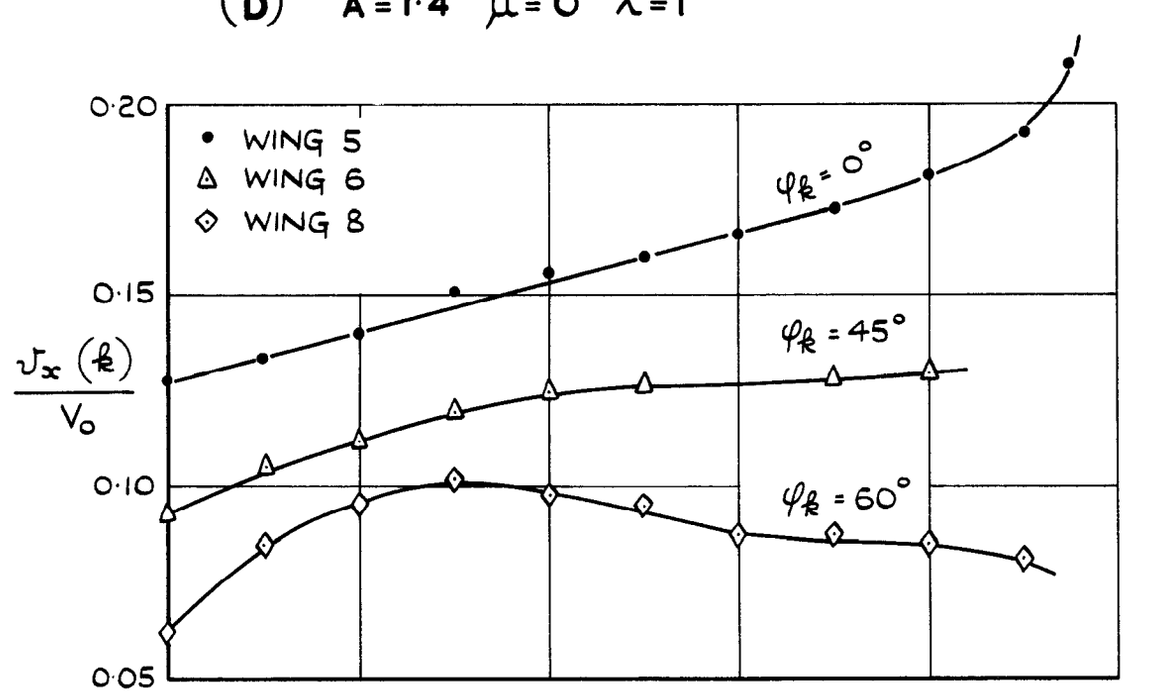

(c) A = 2·8 μ = 1 λ = 0

FIG. 21 (a-c) WINGS 5, 6 & 8 EFFECT OF SWEEP ON VELOCITIES AT MAXIMUM THICKNESS
$\alpha = 0°$

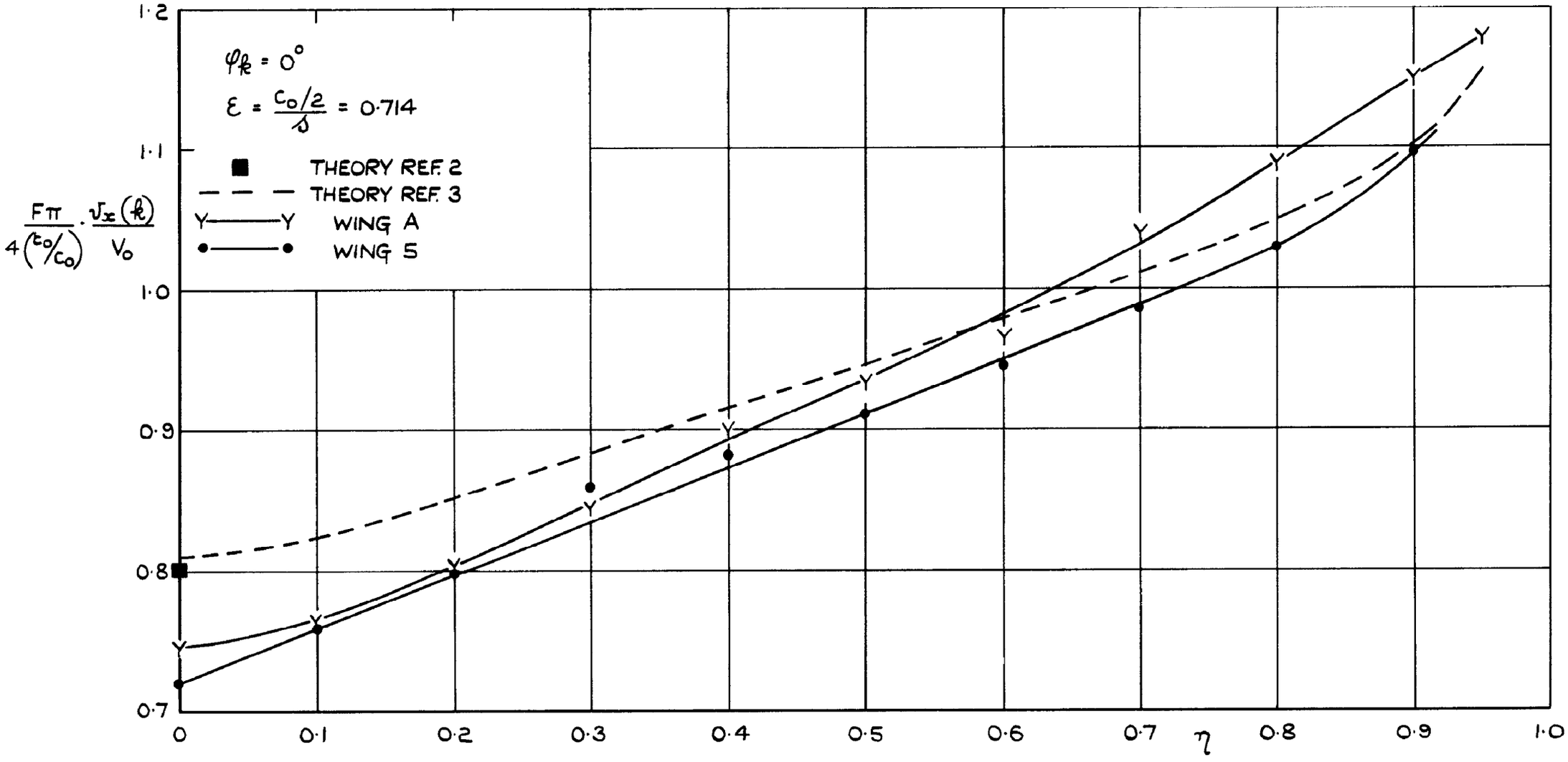

FIG. 22. SUPERVELOCITIES AT MAXIMUM THICKNESS – WINGS A AND 5
$A = 2{\cdot}8 \quad \mu = 1 \quad \lambda = 0 \quad \frac{t_0}{c_0} = 0{\cdot}12$

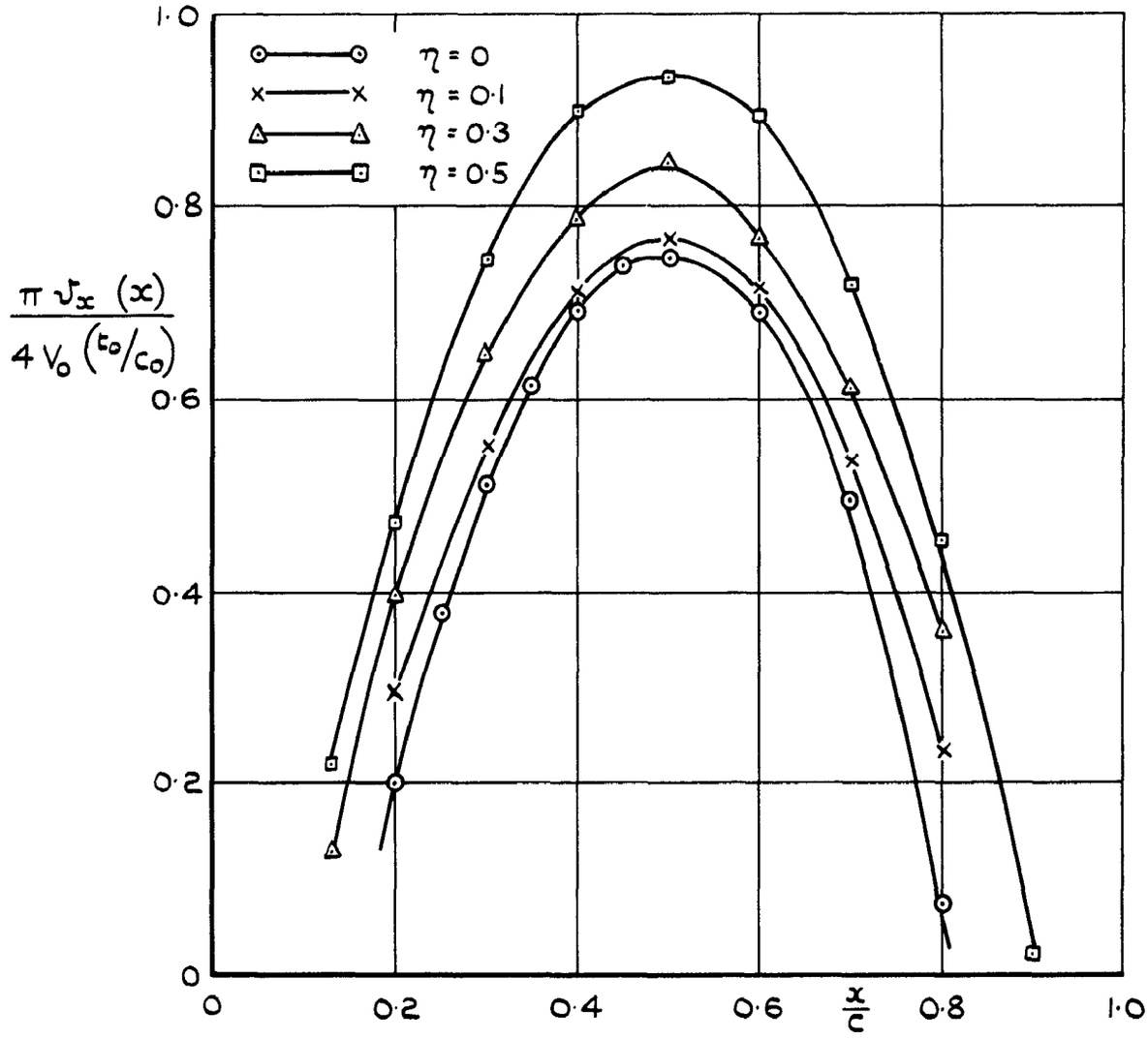

FIG. 23. CHORDWISE DISTRIBUTIONS ON WING A

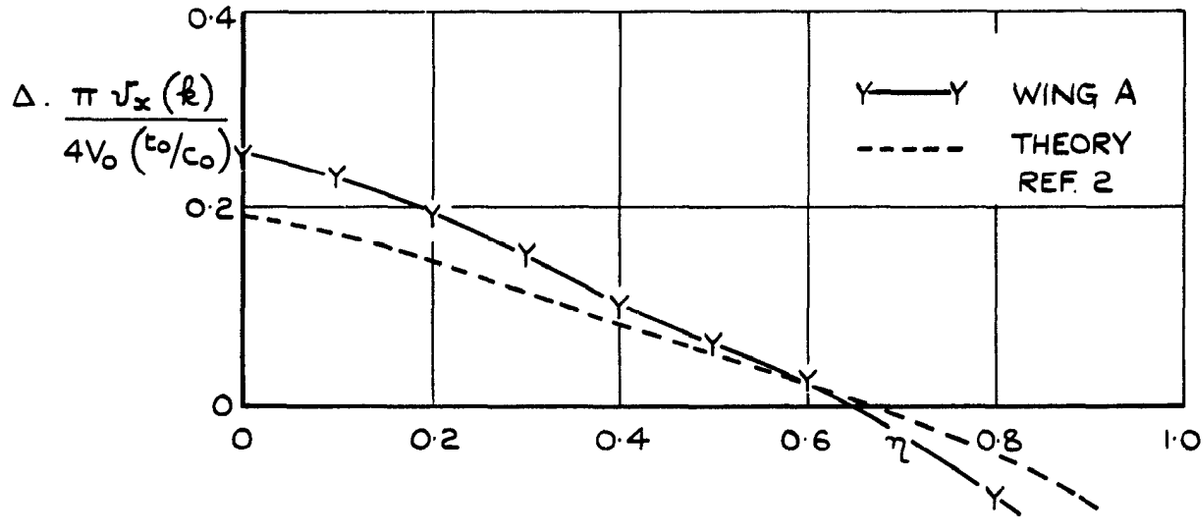

FIG. 24. REDUCTION OF v_x RELATIVE TO TWO-DIMENSIONAL VALUE FOR LOCAL THICKNESS / CHORD RATIO. WING A

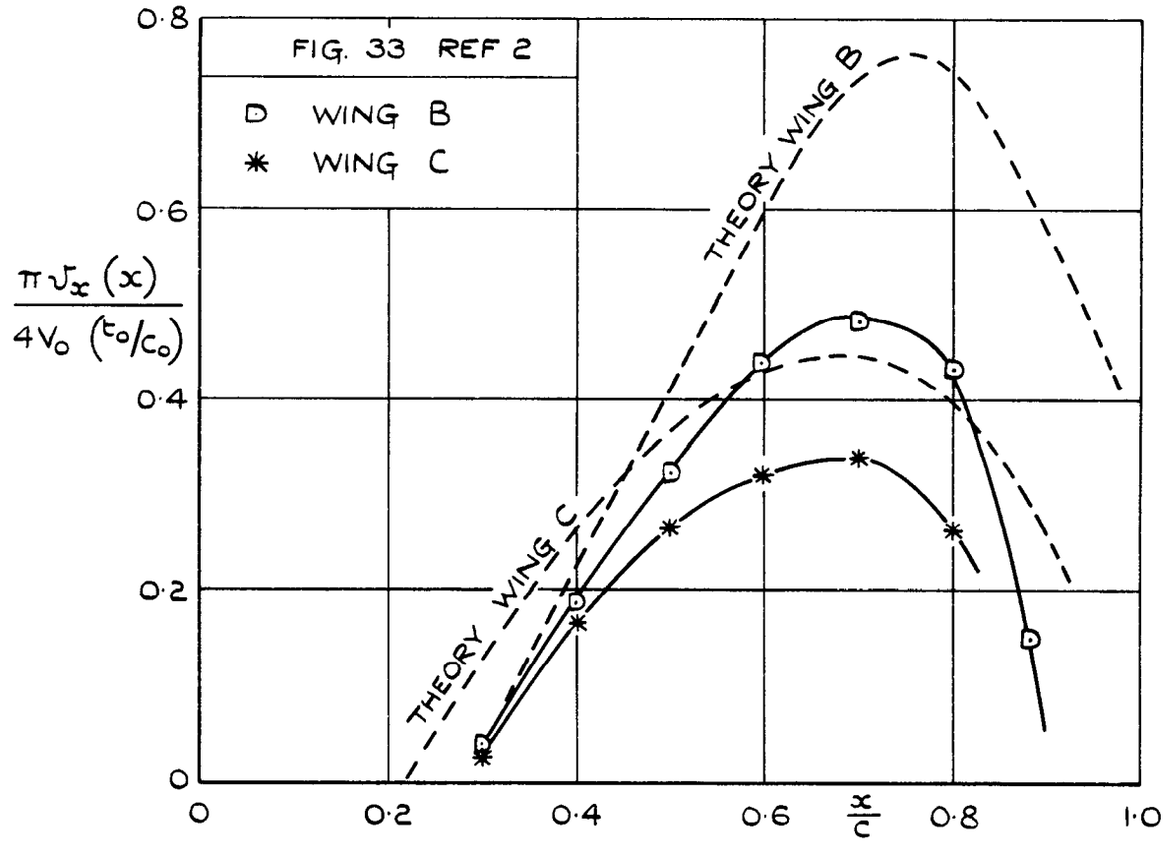

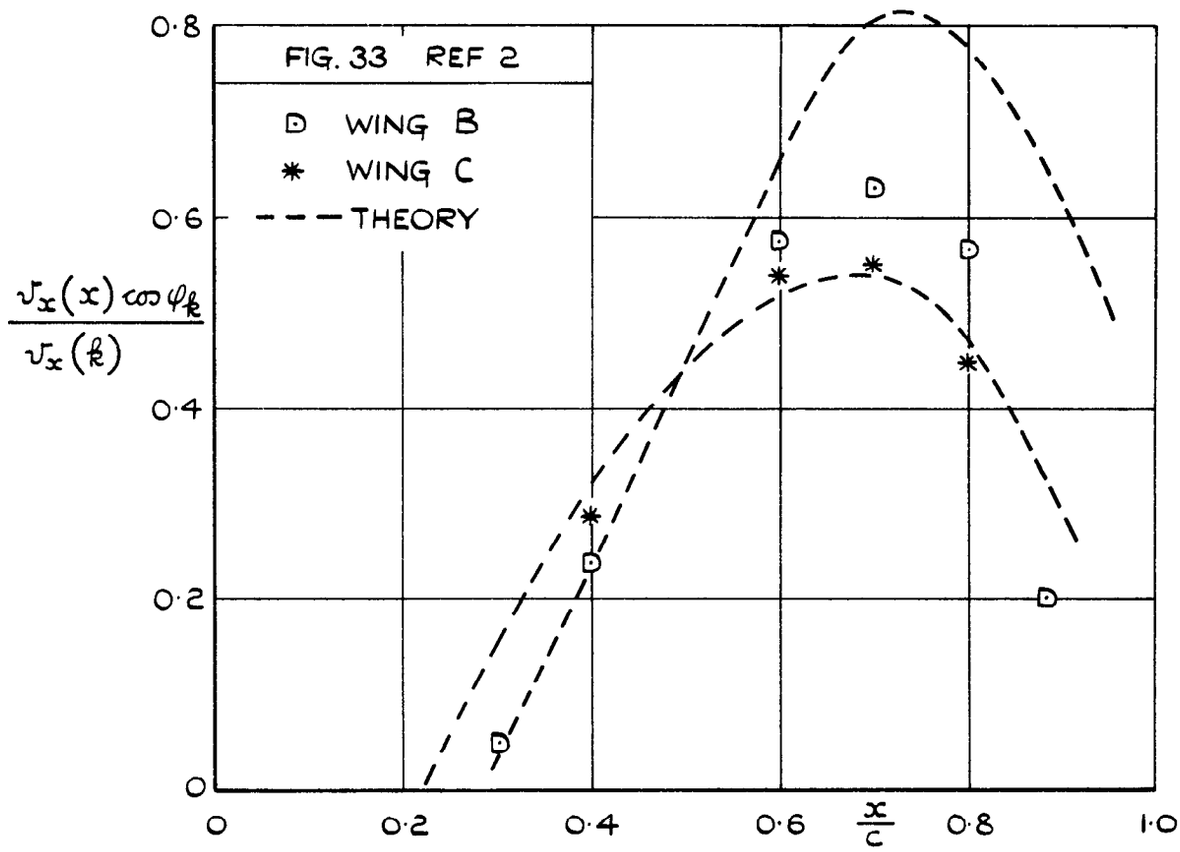

FIG. 25. THEORETICAL AND EXPERIMENTAL SUPERVELOCITY DISTRIBUTIONS ON WINGS B & C. $\eta = 0$
A=1 DELTA.

A.R.C. C.P. No.571

533.693.3:
533.69.031:
533.69.048.2

LOW-SPEED WIND TUNNEL TESTS ON THE EFFECTS OF TAPER ON LOW ASPECT-RATIO WINGS AT ZERO INCIDENCE.
Peckham, D.H. August 1960.

A family of low aspect ratio wings of RAE 101 section, and one of biconvex section, have been tested in the 13 ft x 9 ft low-speed wind tunnel at RAE Bedford.

Results of pressure measurements at zero incidence are analysed to determine the separate effects of low aspect-ratio, thickness taper, planform taper and sweep on the chordwise velocity distributions.

A.R.C. C.P. No.571

533.693.3:
533.69.031:
533.69.048.2

LOW-SPEED WIND TUNNEL TESTS ON THE EFFECTS OF TAPER ON LOW ASPECT-RATIO WINGS AT ZERO INCIDENCE.
Peckham, D.H. August 1960.

A family of low aspect ratio wings of RAE 101 section, and one of biconvex section, have been tested in the 13 ft x 9 ft low-speed wind tunnel at RAE Bedford.

Results of pressure measurements at zero incidence are analysed to determine the separate effects of low aspect-ratio, thickness taper, planform taper and sweep on the chordwise velocity distributions.

A.R.C. C.P. No.571

533.693.3:
533.69.031:
533.69.048.2

LOW-SPEED WIND TUNNEL TESTS ON THE EFFECTS OF TAPER ON LOW ASPECT-RATIO WINGS AT ZERO INCIDENCE.
Peckham, D.H. August 1960.

A family of low aspect ratio wings of RAE 101 section, and one of biconvex section, have been tested in the 13 ft x 9 ft low-speed wind tunnel at RAE Bedford.

Results of pressure measurements at zero incidence are analysed to determine the separate effects of low aspect-ratio, thickness taper, planform taper and sweep on the chordwise velocity distributions.

Published by
HER MAJESTY'S STATIONERY OFFICE

To be purchased from
York House, Kingsway, London w.c.2
423 Oxford Street, London w.1
13A Castle Street, Edinburgh 2
109 St. Mary Street, Cardiff
39 King Street, Manchester 2
50 Fairfax Street, Bristol 1
2 Edmund Street, Birmingham 3
80 Chichester Street, Belfast 1
or through any bookseller

Printed in England

S.O. CODE No.23-9012-71